HHS Public Access

Author manuscript

Biochemistry. Author manuscript; available in PMC 2020 February 12.

Published in final edited form as:

Biochemistry. 2019 February 12; 58(6): 561–574. doi:10.1021/acs.biochem.8b01066.

Nucleotide Excision Repair and Impact of Site-Specific 5',8-Cyclopurine and Bulky DNA Lesions on the Physical Properties of Nucleosomes

Vladimir Shafirovich[*,1], **Marina Kolbanovskiy**[1], **Konstantin Kropachev**[1], **Zhi Liu**[1], **Yuquin Cai**[2], **Michael A. Terzidis**[3], **Annalisa Masi**[3], **Chryssostomos Chatgilialoglu**[3], **Shantu Amin**[4], **Alexander Dadali**[5], **Suse Broyde**[2], and **Nicholas E. Geacintov**[1]

[1]Department of Chemistry, New York University, 31 Washington Place, New York, NY 10003-5180, United States.

[2]Department of Biology, New York University, 31 Washington Place, New York, NY 10003-5180, United States.

[3]Istituto per la Sintesi Organica e la Fotoreattività, Consiglio Nazionale delle Ricerche, Via P. Gobetti 101, 40129 Bologna, Italy.

[4]Department of Pharmacology, Milton S. Hershey Medical Center, Pennsylvania State University College of Medicine, Hershey, PA 17033, United States.

[5]Bronx College of the City University of New York, Bronx, NY 10453, United States.

Abstract

The non-bulky 5',8-cyclopurine DNA lesions (cP) and the bulky, benzo[*a*]pyrene diol epoxide-derived stereoisomeric *cis* and *trans*-N^2-guanine adducts (BPDE-dG) are good substrates of the human nucleotide excision repair (NER) mechanism. These DNA lesions were embedded at the *In* or *Out* rotational settings near the dyad axis in nucleosome core particles reconstituted either with native histones extracted from HeLa cells (HeLa-NCP), or with recombinant histones (Rec-NCP). The cP lesions are completely resistant to NER in human HeLa cell extracts. The BPDE-dG adducts are also NER-resistant in Rec-NCPs, but are good substrates of NER in HeLa NCPs. The four BPDE-dG adduct samples are excised with different efficiencies in free DNA, but in HeLa-NCPs the efficiencies are reduced by a common factor of 2.2 ± 0.2 relative to the NER efficiencies in free DNA. The NER response of the BPDE-dG adducts in HeLa-NCPs is not directly correlated with the observed differences in the thermodynamic destabilization of HeLa NCPs, the Förster Resonance Energy Transfer (FRET) values, or hydroxyl radical footprint patterns, and are weakly dependent on the rotational settings. These and other observations suggest that NER is initiated by the binding of the DNA damage-sensing NER factor XPC-RAD23B to a transiently opened

[*]**Corresponding Author**: V. Shafirovich vs5@nyu.edu Tel: (212) 998-8456 FAX : (212) 995-4205.

Notes

The authors declare no competing financial interests.

Associated Content

Supporting Information

The Supporting Information is available free of charge on the ACS Publications website. Construction of DNA sequences, Relative FRET signal vs [NaCl] plots, Autoradiograph of native gel of XPC binding to NCP (Figures S1-S2) (PDF).

BPDE-modified DNA sequence that corresponds to the known footprint of XPC-DNA-RAD23B complexes (≥ 30 base pairs). These observations are consistent with the hypothesis that post-translation modifications and the dimensions and properties of the DNA lesions are the major factors that have an impact on the dynamics and initiation of NER in nucleosomes.

Table of Contents

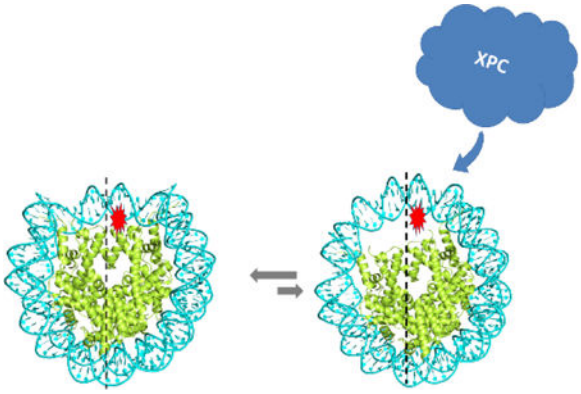

INTRODUCTION

The human nucleotide excision repair (NER) apparatus is an important cellular defense system that excises an astounding variety of structurally diverse DNA lesions.[1] Among examples of NER substrates are bulky DNA lesions like those derived from the binding of metabolically activated polycyclic aromatic hydrocarbons (PAH) to DNA.[2] Certain non-bulky DNA lesions like the oxidatively generated 5',8-cyclopurine adenine (cdA) and guanine (cdG) lesions (Figure 1) are also substrates of NER,[3, 4] but not of base excision repair mechanisms (BER).[5] The relationships between the structural properties of DNA lesions and their susceptibilities to removal by NER mechanisms are of significant interest.[2]

The stereoisomeric 5',8-cyclopurine lesions[6–8] (Figure 1) are formed as a result of chronic infection and inflammation[9] induced by infectious and environmental factors, and are highly mutagenic.[10–15] Some of these lesions have been detected in tissues of experimental animals,[16, 11, 17–20] and humans,[21, 22] and are believed to contribute to human breast and ovarian cancers.[23, 24]

Benzo[*a*]pyrene (B[*a*]P) is a typical PAH that is hydrophobic and practically insoluble in aqueous solutions. However, in mammalian cells it is metabolically activated to the reactive and highly tumorigenic diol epoxide (+)-7R,8,*S*-dihydrodiol, 9S,10*R*-epoxy-benzo[*a*]pyrene (BPDE) intermediate[25–27] to form the covalent and stereoisomeric BPDE-dG DNA adducts[28] shown in (Figure 1; The (+)-*trans*-BPDE-dG adduct shown is positioned in the minor groove of double stranded B-form DNA,[29] while the stereoisomeric (+)-*cis*-adduct adopts a base-displaced intercalated conformation.[30]) Since these are the only BPDE-dG stereoisomeric adducts discussed here, the (+)-sign will be omitted hereafter. If not repaired by the mammalian nucleotide excision repair (NER) system, BPDE-derived DNA adducts can induce mutagenesis and carcinogenesis in laboratory animal[31] and in humans.[32] In cell-

free extracts from human cells, the *trans*- and *cis*- BPDE-dG adducts are excised by the NER system[33] with efficiencies that are similar to those of the NER efficiencies of the 5',8-cyclopurine lesions under the same experimental conditions.[34]

However, it is unknown whether the same relative NER efficiencies prevail at the level of chromatin or nucleosomes, the primary subunits of chromatin. It is well established that histone variants,[35] the post-translational modification (PTM) of histones, and their location on the nucleosome[36] can strongly affect the exposure of otherwise occluded DNA sequences.[37, 38] The accessibilities of DNA sites to other proteins, including Base Excision Repair (BER)[39] and Nucleotide Excison Repair (NER) factors[40] are thus enhanced by these modifications. Both bulky and non-bulky DNA lesions embedded in nucleosomes are less accessible to NER proteins and the efficiencies of NER are therefore reduced relative to free, or naked DNA.[41–43]

In this work, we investigated how DNA lesions of different structure, stereochemistry or bulkiness perturb some of the key physical properties of nucleosomes that might affect their processing by the mammalian NER mechanism. In order to assess differences in NER efficiencies in nucleosomes with and without PTM, the same lesions were embedded in nucleosomes reconstituted either from recombinant (Rec) histones without PTMs, or in native histones derived from human HeLa cells with unspecified post-translational modifications or histone variants. The effects of solvent exposure were examined by positioning the same lesions either at the *In* or *Out* rotational settings adjacent to the nucleosome dyad axis where the repair of lesions has been shown to be most inhibited.[36]

As a first step of understanding the NER response of structurally distinct DNA lesions in intact cells, it is of interest to determine the impact of the histone environment at the level of the single nucleosome on the accessibility and repair of the structurally very different bulky BPDE- dG and non-bulky 5',8-cyclopurine DNA lesions. In this work, we compared the impact of the lesions on the thermodynamic stabilities, hydroxyl radical-induced footprints, and dynamics of nucleosomes measured by Förster Resonance Energy Transfer (FRET) methods. The lesions were positioned at the (*In*), and the more solvent-accessible (*Out*) nucleosome rotational settings (Figure 2).

While the 5',8-cyclopurine- and BPDE-derived DNA lesions in free DNA are good NER substrates, the non-bulky cdA and cdG lesions embedded at either *In* or *Out* rotational settings of native HeLa histone nucleosomes are completely resistant to NER in human cell extracts. By contrast, the excision of the *trans*- and *cis*-BPDE-dG adducts that are excised at different rates in free DNA, is reduced by the same factor of ~ 2.2 in HeLa nucleosomes, and by a factor of ~ 11 in recombinant histone nucleosomes. These findings are compared to the impact of these different DNA lesions on the thermodynamics of formation of the nucleosomes, hydroxyl radical footprints, and nucleosome dynamics evaluated by the FRET method.

MATERIALS AND METHODS

Materials.

The oligonucleotides were purchased from Integrated DNA Technologies (Coralville, IA). All oligonucleotides were purified by gel electrophoresis and isolated by ethanol precipitation. The 208 bp DNA fragment from the *Lytechinus variegatus* 5S RNA gene was purchased from New England Biolabs (Ipswich, MA) and amplified by PCR methods.

Synthesis of Oligonucleotides Containing Single 5',8-Cyclopurine or *trans*-and *cis*-BPDE-dG Lesions.

Phosphoramidites of the four different nucleosides of *R* and *S* cdA and cdG (Figure 1) were prepared following the hydroxyl radical-based protocols.[45, 46] Site-specifically modified 17-mer sequences 5'-d(CCACCAAC[X]CTACCACC) with X = 5'-*R*- or 5'-*S*– cdG/cdA were synthesized and purified following published methods.[47, 48] The *cis*- and *trans*-BPDE-dG adducts (X') embedded in the 11-mer sequence 5'-d(CCTACX'CTACC) were generated by a direct synthesis method and purified as described in detail earlier.[49]

Preparation of 147-mer Duplexes for Reconstitution with Histone Octamers to Form Nucleosome Core Particles (NCP).

The 147-mer ^{32}P-internally labeled (or 5'-endlabeled) modified and unlabeled fully complementary strands (with the canonical C opposite the BPDE- dG and cdG lesions, and T opposite the cdA lesions) were prepared by the phosphorylation/ligation method[33] as described in Supporting Information (Figure S1). The 147-mer duplexes were equivalent to the Widom 601 strong positioning DNA sequence,[50] except for the 17- or 11-mer duplexes containing the BPDE-dG adducts or cdG/cdA lesions termed 601^{cP} or 601^{BP}, respectively. The 17- or 11-mer duplexes were inserted into the 147-mer by replacing an equal number of 601 nucleotides so that the lesions were positioned at the 66-th or 70-th position counted from the 5'-end of the 147-mer, corresponding to the *Out* or *In* rotational settings (Figure 2) at the (superhelical positions SHL = 0.5 and 1.0, respectively. The lesions positioned at "*In*" rotational settings (the 4th (modified) nucleotide on the 5'-side of dyad) faced the histone octamer while those at the "*Out*" position (the 8th (modified) nucleotide faced the aqueous solution environment).

Refolding of Histone Octamers.

The human recombinant histones H2A (Genbank accession number: AAN59960), H2B (AAN59961), H3.1 (AAN10051) and H4 (AAM83108) were purchased from New England Biolabs (Ipswich, MA); the HeLa cell histones were isolated from HeLa cell lysates and purified into two separated fractions of [H2A-H2B] heterodimers and $[H3\text{-}H4]_2$ tetramers using Histone Purification Kit 40025 from Active Motif (Carlsbad, CA). The histone octamers were assembled following the protocol of Luger et al.[51, 52] The integrity of histone octamers was confirmed by SDS-PAGE[53] and MALDI-TOF/MS in the positive mode.[54]

Nucleosome Reconstitution.

The nucleosomes were assembled from the recombinant, or HeLa cell histone octamers and 147-mer 601^{cP} and 601^{BP} duplexes by the gradual dialysis method using the double-dialysis procedure of Lowary and Widom.[55]

Hydroxyl Radical Footprinting of Nucleosomes.

The footprinting experiments were performed with nucleosomes assembled from 5'–^{32}P-labeled DNA and histone octamers as described previously.[56, 57]

Impact of Lesions on the Thermodynamics of Nucleosome Assembly.

A competitive DNA–histone octamer reconstitution method was used to evaluate the effects of the DNA lesions on the thermodynamic stabilities of nucleosomes.[58, 55] Aliquots of histone octamers were added to ~20 pmol unlabeled 208 bp fragment of the 5S RNA gene (competitor DNA) spiked with duplexes containing 5'–^{32}P-endlabeled 601^{cP}, 601^{BP} 147-mer sequences with or without the lesion (the latter constitute the reference DNA) in a 40 μL micro dialysis button system. The nucleosomes were prepared by the double-dialysis method.[55] The distribution of ^{32}P between free and nucleosomal DNA was assessed by native 5% PAGE in 0.3×TBE buffer and analyzed by gel autoradiography. The equilibrium constant was defined as $K = \mathrm{DNA_{NCP}}/\mathrm{DNA_{Free}}$, where $\mathrm{DNA_{NCP}}$ and $\mathrm{DNA_{Free}}$ are quantities of tracer DNA bound to the histone octamers, or free DNA, respectively. The changes in free energies induced by single DNA lesions embedded in 147 bp modified 601 DNA sequences was calculated relative to the unmodified reference 147 bp 601 DNA, $\Delta\Delta G^\circ = -RT \ln(K^{\mathrm{DNA}*}/K^{\mathrm{DNA}})$, where DNA* denotes DNA 147-mer duplexes that contain a single lesion, and DNA denotes the same, but unmodified duplex.[58, 59, 55] This method was successfully used by Mann et al.[48] to explore the effects of DNA damage in nucleosomes induced by BPDE or by UV light.

FRET Assays.

The oligonucleotides containing internal Cy3 and Cy5 dyes were purchased from Integrated DNA Technologies (Coralville, IA) and incorporated into 147-mer 601^{cP} and 601^{bp} DNA sequences with or without the lesions, were prepared by phosphorylation/ligation methods (the details are described in Figure S1, Supporting Information). The fluorescence of Cy3 and Cy5 was excited with vertically polarized ~200 μW green (520 nm) and ~300 μW red (635 nm) light beams of diode lasers, respectively. The fluorescence emission signals were measured at the magic angle (54.7°) relative to the vertical polarization of the laser light, as recommended by Clegg.[60] The intensity of FRET emission ($F^{\mathrm{FRET}}_{670,520}$) was calculated by the well-established equation:[60]

$$F^{FRET}_{670,520} = F^{DA}_{670,520}\left(1 - F^{D}_{670,520}/F^{D}_{565,520} - F^{A}_{670,520}/F^{A}_{670,635}\right) \quad (1)$$

where subscripts denote the emission and excitation wavelengths of the Cy3 (donor, D) and Cy5 (acceptor) dyes. The internal Cy3 and Cy5 labels were positioned at nucleotides 43 and 39 counted from the dyad axis in opposite strands depicted in Figure 2. Thus, in the

nucleosomes, Cy3 and Cy5 are separated by 81 bp, a distance that provides robust FRET signals.[61–66]

The relative stabilities of nucleosomes with and without lesions were determined by measuring the FRET signals as a function of increasing NaCl concentration. The relative FRET efficiencies at particular NaCl concentrations (E) were calculated relative to the E_o value at a low (50 mM) salt concentration, [NaCl]0:

$$E/E_0 = \left(F^{FRET}_{670,520}/F^{DA}_{670,635}\right)/\left[\left(F^{FRET}_{670,520}\right)_0/\left[\left(F^{DA}_{670,635}\right)_0\right]\right] \quad (2)$$

where $E0$ defines the FRET value for fully wrapped NCPs and E for partially unwrapped NCPs.

The relative stabilities of nucleosomes containing single, different lesions were determined by plotting E as a function of salt concentration, [NaCl]. These titration plots were approximated by a sigmoidal function:[67]

$$E/E_0 = 1/\left(1 + \exp\left(\left([\mathrm{NaCl}]_{1/2} - [\mathrm{NaCl}]\right)/a\right)\right) \quad (3)$$

where $[NaCl]_{½}$ is the NaCl concentration at the $E/E_0 = 0.50$ midpoint and a is the slope of the curve at that concentration. The salt concentration at this midpoint is a common measure of the relative stabilities of different nucleosomes.[68, 69]

Nucleotide Excision Repair Assay.

For the NER experiments, the 17-mer or 11-mer sequences containing the cdA/cdG or BPDE-dG lesions, respectively, were 5'–^{32}P-endlabeled before the assembly of the 147-mer 601^{cP} and 601^{BP} DNA sequences for recovering radioactively labeled NER dual incision products. The HeLa S3 cells were purchased from the American Type Culture Collection (Manassas, VA, USA) and the cell extracts were prepared by standard protocols by cell lysis and ammonium sulfate precipitation following published methods.[70–72] The cell extract DNA repair assays and the recovery of the ~ 24–30 nucleotide long dual incision products were conducted as described in detail elsewhere.[72] These dual incision products are the hallmark of successful NER activity[73, 74] and are easily resolved from the 147-mer unreacted oligonucleotides by denaturing 12% polyacrylamide gel electrophoresis. The yield of dual incision products was determined from densitometry tracings of the gel autoradiographs.

RESULTS

Full NER Resistance of 5',8-Cydopurine Lesions in Nucleosomal DNA.

While all four of the 5',8-cyclopurine lesions embedded in free 601^{cP} DNA sequences are excised in HeLa cell extracts, there is no discernable NER activity when the same lesions are embedded at the *In* or *Out* rotational settings in nucleosomes reconstituted with either native

HeLa or recombinant histones (Figure 3A). The full NER resistance of cyclopurine lesions in nucleosomes indicates that the HeLa-NCPs as well as Rec-NCPs remain intact during the incubation in HeLa cell extracts (Figure 3A). No decomposition (or significant repair activity) is evident in most of the Rec-NCPs with BPDE-G adducts either (Figure 3B). These results indicate that the repair of the nucleosomal DNA in cell free extracts can occur without the full disruption of the nucleosome structure as suggested by previous publications on the repair of DNA lesions embedded in nucleosomes.[41, 75, 76, 42, 43, 77] Furthermore, it has been shown that key NER factors such as XPC, XPA and RPA form complexes with nucleosomes without dissociating the histone octamers from the DNA molecules.[41, 78]

The Stereoisomeric BPDE-dG Adducts in Free 601^{BP} HeLa Nucleosomes Are Excised with Different Rates.

In parallel experiments conducted with BPDE-dG adducts, robust NER excision activities were observed in 601^{BP}HeLa cell NCPs (Figure 3B).

Kinetics of Excision.

The relative kinetics of formation of dual incision products are linear in each case up to at least 45 minutes after the start of the incubation in HeLa cell extract (Figure 4B). Each normalized data point reflects the average of three independent experiments (Figure 4). The kinetics of appearance of NER products (relative rates) were evaluated from the slopes of the linear plots shown in Figure 4B and are summarized in Table 1.

NER Excision Rates in HeLa Histone NCPs Relative to the Rates in Free DNA.

As shown earlier, the NER activities in free DNA depend on the *cis*- and *trans*-stereochemistry[33, 79] and also on the DNA sequence context.[72, 80, 81] The relative NER rates observed with HeLa histone NCPs containing *cis*- and trans-stereoisomeric BPDE-dG adducts at the *In* or *Out* rotational setting are reduced by the common factor of 2.2 ±0.3 in HeLa histone NCPs relative to free DNA, regardless of BPDE-dG adduct stereochemistry or rotational setting (Table 1).

Impact of Rotational Setting on NER Activity.

The *Out/In* NER excision ratios for each adduct are similar in free DNA and in HeLa NCPs with values of ~ 1.10(0.94) in the case of the *trans*- and ~0.83(0.83) in the case of the *cis*-BPDE-dG adducts in HeLa NCPs (the numbers in parentheses represent the free DNA values). In recombinant NCPs, the NER efficiencies at the *Out* position are ~11 times smaller than in free DNA, while no NER activity is observable when the same adducts are positioned at the *In* rotational setting (Table 1, and Figures 4B - 4E). It is noteworthy that in recombinant histone NCPs, a small NER activity is observable only at the *Out,* but not at the *In* rotational setting, while in HeLa NCPs the differences are small and not conclusive (~ 10 – 20% smaller yields at *In* rotational settings).

DNA Footprinting Results.

Hydroxyl radical footprinting experiments[56, 57] were performed in order to determine whether the bulky and non-bulky DNA lesions perturb the rotational settings of nucleosomal

DNA to different extents. The autoradiographs of hydroxyl radical footprints and the corresponding scans obtained with *S* cdA lesions embedded in HeLa NCPs shown in Figures 5 demonstrate the same phasing patterns as in the nucleosomal unmodified DNA.[56, 57, 66.] The lack of impact of the non-bulky 5',8-cyclopurine lesions on the rotational settings of nucleosomes is not unusual since the UV photoproducts CTD[75] and (6–4) photoproducts[76] embedded in nucleosomes also do not have a significant impact on the nucleosomal rotational settings.

The overall hydroxyl radical cleavage patterns of BPDE-dG adducts in HeLa NCPs are not significantly different at the *In* (Figures 6A - 6D) and the *Out* (Figures 6E - 6F) rotational settings.

While the rotational settings on the 3'-side of the *In* BPDE-dG adducts are not significantly affected relative to unmodified DNA (Figures 6C - 6D), the modified guanine and 3'-adjacent cytosine-sites are more strongly cleaved than the analogous sites in the unmodified DNA sequence. This observation suggests that the backbone is more solvent-exposed at these two sites in the HeLa histone NCPs. On the 5'-side of the adduct, one nucleotide appears to be missing; this effect arises because the strand break at the site of the modified guanine removes the equivalent of almost two nucleotides (the mass of the BPDE residue (302 Da) is approximately equal to the mass of 2'-deoxyguanosine residue, 283 Da). On the 5'-side of the *In* adducts, the maxima in the scans (Figure 6C - 6D) are slightly shifted by about 4 – 5 nucleotides. In the case of the same adducts at the solvent-exposed *Out* position, there is no enhancement in cleavage of the backbone at the site of the BPDE-modified nucleotide and its 3'-adjacent sites (Figures 6E - 6F), since there are no striking enhancements in the cleavage efficiencies as there are in Figures 6C - 6D in the case of the same adducts at the *In* rotational setting.

Impact of DNA Lesions on the Free Energies of Formation of Nucleosomes.

The free energy change of nucleosome formation containing a DNA lesion is:

$$\Delta\ \Delta\ G = RT\left(\ln K^{DNA*} - \ln K^{DNA}\right) = \ \Delta\ G(DNA + \text{ lesion }) - \ \Delta\ G(\text{ unmodified } DNA) \quad (4)$$

where DNA* denotes nucleosomal DNA with a single 5',8-cyclopurine or BPDE-dG adduct. The free energy difference $\Delta\Delta G$ is a positive quantity if the lesions destabilize the DNA ($K^{DNA*} < K^{DNA}$).

5',8-Cyclopurine Lesions.

The experimental values of AAG(cdG/cdA) indicate that in all cases (except *R* cdA), the $\Delta\Delta G$(cdG/cdA) values are ~ 4–5 times greater, and thus more destabilizing at the *In* than the *Out* locations of HeLa NCPs (Figure 7A). These $\Delta\Delta G$ values Except for the *Out trans-BPDE*-dG adduct, the $\Delta\Delta G$ values are in the range of ~ 0.70 – 0.75 kcal/mol in the case of the other three BPDE-dG adducts in HeLa NCPs (Figure 7B). It is noteworthy that the $\Delta\Delta G$ values are rather similar in HeLa-NCPs and Rec-NCPs, although the NER rates are very different (Figures 3 and 4).

The bulky BPDE-dG adducts are less destabilizing than the 5′,8-cylopurine lesions at the *In* rotational settings. There is a significant difference between $\Delta\Delta G$(cdA/cdG) and $\Delta\Delta G$(BPDE-dG) values at the *In* and *Out* rotational settings. There is a ~ 5-fold differences in the case of the 5′,8-cyclopurine lesions in the HeLa NCPs (Figure 7A), while it is significantly smaller in the case of the BPDE-dG adducts (Figure 7B). These differences in thermodynamic free energy of formation do not seem to be correlated with differences in NER dual incision activities.

Nucleosome Stabilities Probed by FRET Methods.

A representative set of fluorescence emission spectra of Cy3-Cy5-labled unmodified DNA NCPs at different NaCl concentrations are shown in Figure 8A; the addition of NaCl decreases the Cy5 FRET signal at 670 nm and is correlated with the growth of the Cy3 fluorescence at 565 nm.

The FRET ratios obtained with cdG, cdA lesions, and unmodified 601^{cP} in HeLa histone NCPs are plotted in Figures 8B and 8C. Fits of Eq. 3 to the unmodified DNA-NCP data points yield the [NaCl] 1/2 value of 0.85 M (Figure 8D), in good agreement with published values.[68] Similar values were obtained with *S* cdG and *S* cdA lesions positioned at the *Out* rotational settings. However, the stabilities ([NaCl]1/2 values) of the same lesions positioned at the *In* rotational settings are significantly lower (~ 0.6 M, Figure 8D); these results are consistent with the thermodynamic destabilization since the $\Delta\Delta G$ values are ~ 0.8 kcal/mol greater at the *In* than the *Out* rotational settings in the case of cdG and *S* cdA lesions (Figure 7A). In the case of the *R* cdA lesion this difference is less pronounced (Figure 8D and Supporting Information, Figure S2).

In the case of the *cis*- and trans-BPDE-dG adducts, $\Delta\Delta G^{Out} > \Delta\Delta G^{In}$ in the case of the *cis*-,as well as the *trans*-adducts in Rec-NCPs (Figure 7B). The somewhat smaller FRET [NaCl]1/2 values at the *In* than the *Out* settings are qualitatively consistent with this trend (Figure 9C). Similar differences are observed in the case of the same adducts embedded in HeLa NCPs, since the differences in the FRET signals at the *In* and *Out* settings are more pronounced (Figure 9D). Furthermore, there is no correlation with the $\Delta\Delta G^{Out}$ and $\Delta\Delta G^{In}$ values (Figure 7B) as there is in the case of the Rec-NCPs. A clue to these differences are the small, but consistently higher FRET values at the BPDE-dG *Out* rotational settings than the unmodified DNA NCP [NaCl]1/2 values in Rec- and HeLa NCPs (Figures 9C and 9D). Such differences are not observed in the case of the 5′,8-cyclopurine lesions embedded in HeLa NCPs since the [NaCl]1/2 values in HeLa NCPs at the *Out* rotational settings are identical to those in unmodified DNA HeLa NCPs (Figure 8D). As discussed below, intermolecular Van der Waals and other electrostatic interactions that depend on the size and shape of the DNA lesions may contribute to the differences in the thermodynamic $\Delta\Delta G$ destabilization of nucleosomes that are also reflected in the measured FRET [NaCl] 1/2 values.

DISCUSSION

The availability of two families of robust NER substrates with very different physical dimensions allowed us to investigate potential relationships between nucleosome stabilities

determined by equilibrium thermodynamic approaches and FRET methods, rotational settings, and the impact of post-translation modification on NER excision efficiencies. All DNA lesions were placed close to the dyad axis where they are expected to exert the greatest impact on repair and thermodynamic stabilities, especially at the *In* rotational settings. By selecting the 601 strong positioning sequence and 147-mer duplexes, the sliding mechanism of exposure of DNA sequences on NER was eliminated as a possibility.

Previous NER Studies of Defined, Site-Specifically Positioned Lesions Embedded in Nucleosomes.

There are relatively few published investigations of this kind. Studies have been conducted with CTD, (6–4)PP, and N-acetylaminofluorene-guanine (AAF-G) lesions embedded near the dyad in native HeLa histone NCPs. Robust NER response was elicited by the six purified NER factors XPC-RAD23B, XPA, RPA, TFIIH, XPG, and XPF-ERCC1).[41, 76, 42, 43] Excision of these lesions by in HeLa histone NCPs occurred with lower efficiencies than in free DNA[41, 43] by factors of 10 (CTD), ~ 5 (AAF-G), and ~ 2.5 ((6–4)-PP). With (6–4)PP lesions embedded in different DNA sequences in mono- and dinucleosome model system, a two-fold lower excision efficiency relative to free DNA was observed by other workers.[76] An important conclusion from studies using purified NER factors is that the presence of chromatin remodeling factors is not essential for observing NER dual incisions of lesions in nucleosomal DNA *in vitro.* However, the remodeling factors SWI/SNF and ACF did stimulate the removal of AAF-G adducts in nucleosomes by a factor of ~1.5[42], while the ATP-dependent factor ACF enhanced the removal of (6–4)PP lesions by a factor of ~ 2.[76] Other mammalian cell extract NER studies of DNA lesions embedded in nucleosomes include CTD in the strong positioning TG DNA motif,[75] and the cisplatin-derived intra-strand cross-linked GTG-Pt and GG-Pt DNA lesions.[83,77]

Structural Features and NER Response of the 5',8-Cyclopurines in Free DNA.

The cdA and cdG lesions are characterized by intranucleotide cross-links between the C8 purine and the 5'-deoxyribose residue (Figure 1). These oxidatively generated DNA cross-links significantly distort the local DNA duplex structure by constraining the relative orientations of these two residues.[84–86, 34, 87] Structural changes include an abnormal O4'-sugar pucker, an over twisting of the 5',8-cyclopurine: dC (or dT) base pair, a widening of the minor groove, a decrease in local base-base stacking interactions, and weakened *S*-cdG:dC base pairing at the sites of the lesions. Molecular Dynamic Simulation studies suggest that the basic structural and dynamic features of *R* and *S* cdG lesion are carried over to the nucleosomal environment.[87]

DNA Conformations and NER Response of BPDE-dG lesion in Free DNA.

The bulky *trans*-BPDE-dG adducts are positioned in the minor-groove of DNA with all base pairs remaining intact;[29] by contrast, the *cis*-BPDE-dG adduct assumes a base-displaced intercalative conformation that significantly distorts the local base pairs and DNA structure.[88] The relative NER rates of *cis* or *trans* adducts in free DNA depend not only on adduct stereochemistry,[33, 89] but also on the local and more distant base sequence context.[90, 72, 81] Therefore, the relative NER excision efficiencies of the *cis*- and *trans*-BPDE-dG adducts at the two different rotational settings in free DNA are different from one another (Figure 4).

The 5',8-Cydopurine Lesions Affect the Physical Characteristics of HeLa Histone NCPs but NER Activity Is Absent.

The cdA and cdG lesions, although small in bulk, cause significant thermodynamic destabilization and lowering of the FRET [NaCl]1/2 NCP stabilities at the *In,* but not *Out* rotational settings (Figures 7A, and 8, respectively). However, within the experimental uncertainties, the hydroxyl radical footprints at the *In* and *Out* rotational settings are not distinguishable (Figure 6). At the physiologically relevant NaCl concentrations (< 200 mM), the FRET values are up to ~ 20% lower relative to unmodified DNA NCPs at the *In* rotational settings (Figures 8B,C and Figure S2, Supporting Information). Nevertheless, there is no detectable NER activity (Figure 3A). By contrast, the UV light-induced CTD and (6–4)PP lesions are excised by NER mechanisms in mammalian cell extracts.[41, 75, 76, 43, 82] Similar FRET values (lowered by 9–16% relative to unmodified DNA NCPs) were observed with these lesions embedded in the 601 DNA sequence near the dyad in native histone NCPs.[66]

Thermodynamic Destabilization of NCPs by DNA Lesions is not Directly Correlated with the NER Response.

In three out of four cases, the $\Delta\Delta G^{In}$ and $\Delta\Delta G^{Out}$ values are not significantly different from one another in the case of the *cis*- and *trans*-BPDE-dG adducts in Rec-NCPs and in HeLa-NCPs (Figure 5B). However, the NER activities are entirely absent at the *In*, and very low at the *Out* rotational settings in recombinant histone NCPs, while relatively strong NER activities are observed in HeLa-NCPs (Figure 4).

5',8-Cyclopurine Lesions can be More Destabilizing than BPDE-dG Adducts.

At the *In* rotational setting the non-bulky cdA and cdG lesions are more destabilizing than the bulky BPDE-dG adducts. However, at the Out setting, the BPDE-dG adducts are more destabilizing. These observations suggest that non-covalent Van der Waals and other electrostatic interactions between the bulky hydrophobic aromatic ring systems of BPDE and adjacent histone residues might counteract the destabilizing impact of structural distortions caused by the bulky DNA adducts, thus accounting for the smaller $\Delta\Delta G^{In}$ values. This conclusion is consistent with the findings of Mann et al.[54] who found earlier that randomly BPDE-modified (with an average of one randomly positioned adduct per nucleosome particle) 146-mer *Xenopus borealis* 5S rRNA gene fragment DNA give rise to a small, overall nucleosome-stabilizing effect with $\Delta\Delta G \approx$ - 0.30 kcal/mol.

NER Dual Excision Ratios at *In* and *Out* Settings are Different from Normal Patterns Observed in Base Excision Repair Assays.

The removal of non-bulky lesions (e.g., uracil, thymine glycol, 8-oxoG, and abasic sites) by BER mechanisms has received significant attention.[91, 36, 92, 93, 39] While exceptions have been noted,[91, 94–96] BER substrates are excised more efficiently when positioned at the *Out* than the *In* rotational settings.[97, 91, 98–100, 39] However, there are few analogous studies of NER activities. In the case of the non-bulky CTD UV photoproducts, an *Out/In* ratio of ~ 1.5 was reported for the NER in mammalian cell extracts embedded in the strong positioning TG motif DNA near the dyad in native chicken erythrocyte histone nucleosomes.[82]

The very slow rate of NER observed in the case of *cis*-and *trans*-BPDE-dG adducts in Rec-NCPs, and the absence of NER signals at the *In* settings, is qualitatively consistent with an *Out* > *In* trend of excision efficiencies (Figure 4B). In the case of the *cis*-and *trans-BPDE*-dG adducts in HeLa-NCPS, the *Out/In* ratios are 1.2 and 1.1, respectively (Table 1). The intrinsic *Out/In* ratios in free DNA are ~ 0.92 ± 0.02 *(cis*-and trans-BPDE-dG), and thus the difference in the *Out/In* ratios observed in HeLa-NCPs are considered to be small and not definitive in the absence of further examples.

Comparing NER rates of all four different BPDE-dG samples in HeLa histone NCPs, the NER rates are reduced in each case by the common factor of 2.2 ±0.3 (Table 1). Thus, within the approximate ±10 % experimental range, the relative probabilities of excision are similar in free DNA and in HeLa histone NCPs, although the NER efficiencies of the stereoisomeric BPDE-dG in free DNA vary by as much as a factor of 4 (Figure 4A).

The approximately constant proportionalities between NER efficiencies observed in the cases of free and nucleosomal DNA suggest that the nucleosomal environment reduces the probability of NER by a similar factor for all of the different DNA adducts that are repaired with different efficiencies in free DNA. There are no obvious quantitative correlations between NER efficiencies, thermodynamic destabilization and rotational setting. These observations are consistent with a similar extent of exposure of each of the different BPDE-dG adducts to the NER factors that initiate and catalyze the dual incision NER pathway. Since XPC-RAD23B is the first NER factor that recognizes NER substrates and its DNA footprint is ~ 30 base pairs,[101] the lengths of the DNA sequences transiently exposed must be longer than this number of base pairs for efficient XPC-RAD23B binding to occur. Once the lesion-containing DNA sequences are exposed, these observations suggest that the *relative* NER efficiencies of the different DNA adducts parallel those observed in free DNA.

The footprint of XPC-RAD23B (molar mass ~ 180 kDa) is ~ 30 base pairs,[102] and efficient binding requires DNA sequences at least 45 base pairs in length.[103] Therefore, the complete unwrapping of the nucleosome may not be necessary for NER to occur. Indeed, it has been demonstrated that XPC binds to nucleosomal DNA with a lower probability than to free DNA without dissociating the DNA from the histone core.[41, 78] We have reproduced these results and verified that XPC-RAD23B also binds to HeLa histone NCPs with BPDE-dG lesions without the full dissociation of the nucleosomes (Supporting Information)..

Relationships between NER Rates and Nucleosome Unwrapping Phenomena: a Kinetic Model.

The higher rates of NER of BPDE-dG adducts in HeLa histone than in recombinant histone NCPs indicate that the post-translational modification of histones and nucleosome unwrapping dynamics play an important role in the repair of the BPDE-dG but not the 5′,8-cyclopurine lesions. With XPC-RAD23B (abbreviated as XPC), the other abbreviations are NCP_{Closed} , NCP_{open} , and XPC-NCP, represent the protein-accessible, protein-inaccessible NCPs, and XPC-NCP complexes, respectively.

The following sequence of steps is proposed:

$$\left[\mathrm{NCP_{Closed}}\right] \underset{k_2}{\overset{k_1}{\rightleftarrows}} \left[\mathrm{NCP_{Open}}\right] \xrightarrow{k_2[\mathrm{XPC}]} [\mathrm{XPC-NCP}] \rightarrow \mathrm{Excision} \quad (5)$$

The binding of XPC to the nucleosomal DNA depends on the rate constant *k*2. The local unwrapping and rewrapping occur with rate constants k_1 and k_{-1}, respectively, that define the equilibrium constant $K_{eq} = k_1/k_{-1} = [\mathrm{NCP_{open}}]/[\mathrm{NCP_{Closed}}]$. The formation of the XPC-NCP complex leads to the subsequent recruitment of the other NER factors that ultimately results in the formation of the NER excision products (Figure 3). The rate of formation of the [XPC-NCP] complex can be described by the following equation:

$$\frac{d[\mathrm{XPC-NCP}]}{dt} = \frac{k_1 k_2 [\mathrm{XPC}]\left[\mathrm{NCP_{Closed}}\right]}{k_{-1} + k_2[\mathrm{XPC}]} \quad (6)$$

Previous results indicate that the access of XPC to the DNA lesions in HeLa histone NCPs is sterically hindered;[41, 78] however, once the initial XPC-NCP complex is formed, the unwrapped state of the NCP is stabilized by the XPC-DNA complex, thus facilitating the assembly of the other NER factors. The relationship between the equilibrium constant K_{eq} and experimental FRET values is the following

$$K_{eq} = k_1/k_2 = \left(1 - E/E_0\right)/\left(E/E_0\right) \quad (7)$$

This equation was originally developed for describing the unwrapping-rewrapping NCP equilibria at different salt concentrations.[104] In our case, *E0* is the reference FRET value for unmodified DNA ($K_{eq} < 0.1$),[104] while *E* is the value for the same NCP but containing a single DNA lesion. We consider three limiting cases of Eq. 6 that are significant.

Case I.

In the first limit $k_{-1} >> k_2[\mathrm{XPC}]$ and the rate of XPC-NCP formation is proportional to $K_{\mathrm{eq}} k_2[\mathrm{XPC}]$. In this case the rate of repair is directly proportional to the equilibrium constant K_{eq}, and thus to the relative FRET values *E*/*E*0, the bimolecular rate constant *k2* and the [XPC] concentration.

Case II.

In the second limit, $k_{-1} \approx k_2[\mathrm{XPC}]$, the dependence of the XPC binding rate on the measured E/E_0 FRET value will be smaller than in Case I, and will diminish as a function of increasing $k_{-1}/k_2[\mathrm{XPC}]$ ratio.

Case III.

In the third limit, $k_2[\mathrm{XPC}] >> k_{-1}$, and the XPC capture rate (Eq. 6) is proportional to the unwrapping rate constant *k*1, and thus not directly proportional to K_{eq} and the FRET values.

The lack of NER activity of the 5′,8-cyclopurine lesions in HeLa NCPs is surprising since, like BPDE-dG adducts, it is an excellent NER substrate in free DNA. This lack of NER activity suggests that the binding of NER factors to these physically small lesions is sterically hindered by local histone-DNA configurations that interfere with the proper binding and alignment of XPC to the cdA and cdG lesions. Such a mechanism is consistent with Case I, with k-1 >> $k2$[XPC], suggesting that the rate constant $k2$ is small in comparison to the same rate constant in the case of BPDE-dG adducts in the same HeLa histone NCPs.

In the case of BPDE-dG adducts in recombinant histone NCPs, the impact of the adducts on FRET and [NaCl] 1/2 salt destabilization parameters is significantly smaller (Figures 9A,C) than in the case of HeLa histone NCPs (Figure 9B,D). A weak NER activity is observed in the case of the *Out trans*- and *cis*-BPDE-dG adducts in recombinant histone NCPs (Figured 4B,D). However, there is no discernable NER at the *In* rotational setting (Figures 4A,C) in the case of the BPDE-dG adducts. These observations suggest that Case I is applicable to BPDE-dG adducts in Rec-NCPs at the *In* position with k-1 >> $k2$[XPC] with no XPC binding and observable NER activity. At the *Out* position, however, weak NER activity is observable and, k-1 ≤ $k2$[XPC] (case II).

In the case of the *cis*-and *trans*-BPDE-dG adducts positioned either at the *In* or the *Out* rotational settings in HeLa-NCPs, Case III is applicable with $k2$[XPC] > k-1. In this case, the rate of XPC binding is proportional to the unwrapping rate constant k_1, but is not proportional to the equilibrium constant K_{eq}, or the FRET efficiency.

The results obtained by the FRET method (Figure 9D) indicate that on average, the nucleosome dynamics are more enhanced when the BPDE-dG adducts are positioned at the *In* than the *Out* rotational settings. On the other hand, the bulky polycyclic aromatic residues are less exposed to the solvent environment at the *In* than the *Out* rotational setting. However, since robust NER activities are observed in all four cases (Figure 4), the solvent exposure factor seems to play a minor role in the case of the bulky BPDE-dG adducts. The unwrapping/rewrapping phenomena that expose sufficiently long DNA sequences that allow the XPC factor to gain a toehold on the exposed sequences leads to irreversible XPC-DNA complex formation that initiates the recruitment of subsequent NER factors.

CONCLUSIONS

The strong differences in NER activities between post-translationally modified and recombinant histone nucleosomes are consistent with the notion that the NER activities depend on the transient unwrapping and partial exposure of nucleosomal DNA sequences to the NER factor XPC-RAD23B. This notion is consistent with earlier studies that suggest that enhancements in NER activities may be associated with the acetylation of NCPs.[105] Electrophoretic mobility shift assays indicate that the octamer histone core particles are not evicted in the process.[41, 78] The complete NER resistance of the cyclopurine lesions is attributed to the relatively small physical size of the cdG and cdA lesions that is not significantly different from natural nucleotides. In contrast to the larger-sized and bulky BPDE-dG adducts, the 5′,8-cyclopurine lesions do not appear to sufficiently perturb the

local DNA-histone interactions, thus hindering the successful recruitment of the NER factor XPC-RAD23B that initiates the NER process in human cell extracts. This hypothesis is consistent with the structural features deduced from and NMR and molecular dynamics analysis of an *S*-cdG lesion opposite dC in a double-stranded oligonucleotide duplex.[84] While the cdG lesion perturbed the helical twist and base pair stacking at the lesion site and adjacent base pairs, Watson-Crick base pairing and the helical structure of the duplex, though altered, were maintained. This suggests that 8,5'-cyclopurine-containing DNA duplexes might not cause sufficient local perturbations of the histone fold of nucleosomes to elicit the NER response. The robust NER activity observed with the same lesions embedded in free double-stranded DNA (Figure 3A) is attributed to the significant thermodynamic destabilization of double-stranded DNA caused by the 8,5′-cyclopurine lesions.

Supplementary Material

Refer to Web version on PubMed Central for supplementary material.

Acknowledgments

Funding

This work was supported by the NIH National Cancer Institute Grant R01 CA168469 (neg), and in part by the National Institute of Environmental Health Sciences Grants 5R01ES024050 (neg), and R01-ES025987(sb). Components of this work were conducted in the Shared Instrumentation Facility at NYU that was constructed with support from a Research Facilities Improvement Grant (C06 RR-16572) from the National Center for Research Resources, National Institutes of Health. The content is solely the responsibility of the authors and does not necessarily represent the official views of the National Institutes of Health.

ABBREVIATIONS

BER	base excision repair
NER	nucleotide excision repair
PAH	polycyclic aromatic hydrocarbon
NCP	nucleosome particle
SHL	superhelical location
FRET	Fluorescence Resonance Energy Transfer
CTD	cyclobutane thymine dimer
cdA	5′,8-cycloadenine
cdG	5′,8-cycloguanine
BPDE-dG	benzo[*a*]pyrene diol epoxide-derived N^2-guanine adduct
bp	base pair
nt	nucleotide

REFERENCES

(1). Gillet LC, and Scharer OD (2006) Molecular mechanisms of mammalian global genome nucleotide excision repair, Chem. Rev. 106, 253–276. [PubMed: 16464005]

(2). Geacintov NE, and Broyde S (2017) Repair-Resistant DNA Lesions, Chem. Res. Toxicol. 30, 1517–1548. [PubMed: 28750166]

(3). Brooks PJ, Wise DS, Berry DA, Kosmoski JV, Smerdon MJ, Somers RL, Mackie H, Spoonde AY, Ackerman EJ, Coleman K, Tarone RE, and Robbins JH (2000) The oxidative DNA lesion 8,5'-(S)-cyclo-2'-deoxyadenosine is repaired by the nucleotide excision repair pathway and blocks gene expression in mammalian cells, J. Biol. Chem. 275, 22355–22362. [PubMed: 10801836]

(4). Kuraoka I, Bender C, Romieu A, Cadet J, Wood RD, and Lindahl T (2000) Removal of oxygen free-radical-induced 5',8-purine cyclodeoxynucleosides from DNA by the nucleotide excision-repair pathway in human cells, Proc. Natl. Acad. Sci. US A 97, 3832–3837.

(5). Pande P, Das RS, Shepard C, Kow YW, and Basu AK (2012) Repair efficiency of (5'S)-8,5-cyclo-2'-deoxyguanosine and (5'S)-8,5'-cyclo-2'-deoxyadenosine depends on the complementary base, DNA Repair (Amst) 11, 926–931. [PubMed: 23063091]

(6). Chatgilialoglu C, Bazzanini R, Jimenez LB, and Miranda MA (2007) (5'S)-and (5'R)-5',8-cyclo-2'-deoxyguanosine: mechanistic insights on the 2'-deoxyguanosin-5'-yl radical cyclization, Chem. Res. Toxicol. 20, 1820–1824. [PubMed: 17988100]

(7). Brooks PJ (2008) The 8,5'-cyclopurine-2'-deoxynucleosides: candidate neurodegenerative DNA lesions in xeroderma pigmentosum, and unique probes of transcription and nucleotide excision repair, DNA Repair (Amst) 7, 1168–1179. [PubMed: 18495558]

(8). Jaruga P, and Dizdaroglu M (2008) 8,5'-Cyclopurine-2'-deoxynucleosides in DNA: mechanisms of formation, measurement, repair and biological effects, DNA Repair (Amst) 7, 1413–1425. [PubMed: 18603018]

(9). Lonkar P, and Dedon PC (2011) Reactive species and DNA damage in chronic inflammation: reconciling chemical mechanisms and biological fates, Int. J. Cancer 128, 1999–2009. [PubMed: 21387284]

(10). Jasti VP, Das RS, Hilton BA, Weerasooriya S, Zou Y, and Basu AK (2011)(5'S)-8,5'-cyclo-2'-deoxyguanosine is a strong block to replication, a potent pol V-dependent mutagenic lesion, and is inefficiently repaired in Escherichia coli, Biochemistry 50, 3862–3865. [PubMed: 21491964]

(11). Wang J, Yuan B, Guerrero C, Bahde R, Gupta S, and Wang Y (2011) Quantification of oxidative DNA lesions in tissues of Long-Evans Cinnamon rats by capillary high-performance liquid chromatography-tandem mass spectrometry coupled with stable isotope-dilution method, Anal. Chem. 83, 2201–2209. [PubMed: 21323344]

(12). Swanson AL, Wang J, and Wang Y (2012) Accurate and efficient bypass of 8,5'-cyclopurine-2'-deoxynucleosides by human and yeast DNA polymerase eta, Chem. Res. Toxicol. 25, 1682–1691. [PubMed: 22768970]

(13). You C, Dai X, Yuan B, Wang J, Wang J, Brooks PJ, Niedernhofer LJ, and Wang Y (2012) A quantitative assay for assessing the effects of DNA lesions on transcription, Nat. Chem. Biol. 8, 817–822. [PubMed: 22902614]

(14). You C, Swanson AL, Dai X, Yuan B, Wang J, and Wang Y (2013) Translesion synthesis of 8,5'-cyclopurine-2'-deoxynucleosides by DNA polymerases eta, iota, and zeta, J. Biol. Chem. 288, 28548–28556. [PubMed: 23965998]

(15). Pednekar V, Weerasooriya S, Jasti VP, and Basu AK (2014) Mutagenicity and genotoxicity of (5'S)-8,5'-cyclo-2'-deoxyadenosine in Escherichia coli and replication of (5'S)-8,5'-cyclopurine-2'-deoxynucleosides in vitro by DNA polymerase IV, exo-free Klenow fragment, and Dpo4, Chem. Res. Toxicol. 27, 200–210. [PubMed: 24392701]

(16). Kirkali G, de Souza-Pinto NC, Jaruga P, Bohr VA, and Dizdaroglu M (2009) Accumulation of (5'S)-8,5'-cyclo-2'-deoxyadenosine in organs of Cockayne syndrome complementation group B gene knockout mice, DNA Repair (Amst) 8, 274–278. [PubMed: 18992371]

(17). Mitra D, Luo X, Morgan A, Wang J, Hoang MP, Lo J, Guerrero CR, Lennerz JK, Mihm MC, Wargo JA, Robinson KC, Devi SP, Vanover JC, D'Orazio JA, McMahon M, Bosenberg MW, Haigis KM, Haber DA, Wang Y, and Fisher DE (2012) An ultraviolet-radiation-independent

pathway to melanoma carcinogenesis in the red hair/fair skin background, Nature 491, 449–453. [PubMed: 23123854]

(18). Shaked H, Hofseth LJ, Chumanevich A, Chumanevich AA, Wang J, Wang Y, Taniguchi K, Guma M, Shenouda S, Clevers H, Harris CC, and Karin M (2012) Chronic epithelial NF-kappaB activation accelerates APC loss and intestinal tumor initiation through iNOS up-regulation, Proc. Natl. Acad. Sci U S A 109, 14007–14012. [PubMed: 22893683]

(19). Tilstra JS, Robinson AR, Wang J, Gregg SQ, Clauson CL, Reay DP, Nasto LA, St Croix CM, Usas A, Vo N, Huard J, Clemens PR, Stolz DB, Guttridge DC, Watkins SC, Garinis GA, Wang Y, Niedernhofer LJ, and Robbins PD (2012) NF-kappaB inhibition delays DNA damage-induced senescence and aging in mice, J. Clin. Invest. 122, 2601–2612. [PubMed: 22706308]

(20). Wang J, Clauson CL, Robbins PD, Niedernhofer LJ, and Wang Y (2012) The oxidative DNA lesions 8,5'-cyclopurines accumulate with aging in a tissue-specific manner, Aging Cell 11, 714–716. [PubMed: 22530741]

(21). Jaruga P, and Dizdaroglu M (2010) Identification and quantification of (5'R)- and (5'S)-8,5'-cyclo-2'-deoxyadenosines in human urine as putative biomarkers of oxidatively induced damage to DNA, Biochem. Biophys. Res. Commun. 397, 48–52. [PubMed: 20471371]

(22). Jaruga P, Rozalski R, Jawien A, Migdalski A, Olinski R, and Dizdaroglu M (2012) DNA damage products (5'R)- and (5'S)-8,5'-cyclo-2'-deoxyadenosines as potential biomarkers in human urine for atherosclerosis, Biochemistry 51, 1822–1824. [PubMed: 22360777]

(23). Nyaga SG, Jaruga P, Lohani A, Dizdaroglu M, and Evans MK (2007) Accumulation of oxidatively induced DNA damage in human breast cancer cell lines following treatment with hydrogen peroxide, Cell Cycle 6, 1472–1478. [PubMed: 17568196]

(24). Rodriguez H, Jaruga P, Leber D, Nyaga SG, Evans MK, and Dizdaroglu M (2007) Lymphoblasts of women with BRCA1 mutations are deficient in cellular repair of 8,5'-Cyclopurine-2'-deoxynucleosides and 8-hydroxy-2'-deoxyguanosine, Biochemistry 46, 2488–2496. [PubMed: 17288454]

(25). Weinstein IB, Jeffrey AM, Jennette KW, Blobstein SH, Harvey RG, Harris, Autrup H, Kasai H, and Nakanishi K (1976) Benzo(a)pyrene diol epoxides as intermediates in nucleic acid binding in vitro and in vivo, Science 193, 592–595. [PubMed: 959820]

(26). Buening MK, Wislocki PG, Levin W, Yagi H, Thakker DR, Akagi H, Koreeda M, Jerina DM, and Conney AH (1978) Tumorigenicity of the optical enantiomers of the diastereomeric benzo[a]pyrene 7,8-diol-9,10-epoxides in newborn mice: exceptional activity of (+)-7beta, 8alpha-dihydroxy-9alpha,10alpha-epoxy-7,8,9,10- tetrahydrobenzo[a]pyrene, Proc. Natl. Acad. Sci. USA 75, 5358–5361. [PubMed: 281685]

(27). Koreeda M, Moore PD, Wislocki PG, Levin W, Yagi H, and Jerina DM (1978) Binding of benzo[a]pyrene 7,8-diol-9,10-epoxides to DNA, RNA, and protein of mouse skin occurs with high stereoselectivity, Science 199, 778–781. [PubMed: 622566]

(28). Cheng SC, Hilton BD, Roman JM, and Dipple A (1989) DNA adducts from carcinogenic and noncarcinogenic enantiomers of benzo[a]pyrene dihydrodiol epoxide, Chem. Res. Toxicol. 2, 334–340. [PubMed: 2519824]

(29). Cosman M, de los Santos C., Fiala R, Hingerty BE, Singh SB, Ibanez V, Margulis LA, Live D, Geacintov NE, Broyde S, and Patel DJ (1992) Solution conformation of the major adduct between the carcinogen (+)- anti-benzo[a]pyrene diol epoxide and DNA, Proc. Natl. Acad. Sci. U.S.A. 89, 1914–1918. [PubMed: 1311854]

(30). Cosman M, de los Santos C., Fiala R, Hingerty BE, Ibanez V, Luna E, Harvey R, Geacintov NE, Broyde S, and Patel DJ (1993) Solution conformation of the (+)-cis-anti-[BP]dG adduct in a DNA duplex: intercalation of the covalently attached benzo[a]pyrenyl ring into the helix and displacement of the modified deoxyguanosine, Biochemistry 32, 4145–4155. [PubMed: 8476845]

(31). Wijnhoven SW, Kool HJ, van Oostrom CT, Beems RB, Mullenders LH, van Zeeland AA, van der Horst GT, Vrieling H, and van Steeg H (2000) The relationship between benzo[a]pyrene-induced mutagenesis and carcinogenesis in repair-deficient Cockayne syndrome group B mice, Cancer. Res. 60, 5681–5687. [PubMed: 11059760]

(32). Luch A (2005) Nature and nurture - Lessons from chemical carcinogenesis, Nat. Rev.Cancer 5, 113–125. [PubMed: 15660110]

(33). Hess MT, Gunz D, Luneva N, Geacintov NE, and Naegeli H (1997) Base pair conformation-dependent excision of benzo[a]pyrene diol epoxide-guanine adducts by human nucleotide excision repair enzymes, Mol. Cell. Biol. 17, 7069–7076. [PubMed: 9372938]

(34). Kropachev K, Ding S, Terzidis MA, Masi A, Liu Z, Cai Y, Kolbanovskiy M, Chatgilialoglu C, Broyde S, Geacintov NE, and Shafirovich V (2014) Structural basis for the recognition of diastereomeric 5',8-cyclo-2'-deoxypurine lesions by the human nucleotide excision repair system, Nucleic Acids Res. 42, 5020–5032. [PubMed: 24615810]

(35). Soria G, Polo SE, and Almouzni G (2012) Prime, repair, restore: the active role of chromatin in the DNA damage response, Mol. Cell. 46, 722–734. [PubMed: 22749398]

(36). Rodriguez Y, and Smerdon MJ (2013) The structural location of DNA lesions in nucleosome core particles determines accessibility by base excision repair enzymes, J. Biol. Chem. 288, 13863–13875. [PubMed: 23543741]

(37). Anderson JD, Lowary PT, and Widom J (2001) Effects of histone acetylation on the equilibrium accessibility of nucleosomal DNA target sites, J. Mol. Biol. 307, 977–985. [PubMed: 11286549]

(38). Bowman GD, and Poirier MG (2015) Post-translational modifications of histones that influence nucleosome dynamics, Chem. Rev. 115, 2274–2295. [PubMed: 25424540]

(39). Menoni H, Di Mascio P, Cadet J, Dimitrov S, and Angelov D (2017) Chromatin associated mechanisms in base excision repair - nucleosome remodeling and DNA transcription, two key players, Free. Radic. Biol. Med. 107, 159–169. [PubMed: 28011149]

(40). Li S (2012) Implication of posttranslational histone modifications in nucleotide excision repair, Int. J. Mol. Sci. 13, 12461–12486. [PubMed: 23202908]

(41). Hara R, Mo J, and Sancar A (2000) DNA damage in the nucleosome core is refractoryto repair by human excision nuclease, Mol. Cell. Biol. 20, 9173–9181. [PubMed: 11094069]

(42). Hara R, and Sancar A (2002) The SWI/SNF chromatin-remodeling factor stimulates repair by human excision nuclease in the mononucleosome core particle, Mol. Cell. Biol. 22, 6779–6787. [PubMed: 12215535]

(43). Hara R, and Sancar A (2003) Effect of damage type on stimulation of human excision nuclease by SWI/SNF chromatin remodeling factor, Mol. Cell. Biol. 23, 4121–4125. [PubMed: 12773556]

(44). Vasudevan D, Chua EY, and Davey CA (2010) Crystal structures of nucleosome core particles containing the '601' strong positioning sequence, J. Mol. Biol. 403, 1–10. [PubMed: 20800598]

(45). Navacchia ML, Chatgilialoglu C, and Montevecchi PC (2006) C5 '-adenosinyl radical cyclization. A stereochemical investigation, J. Org. Chem. 71, 4445–4452. [PubMed: 16749773]

(46). Terzidis MA, and Chatgilialoglu C (2013) Radical Cascade Protocol for the Synthesis of (5 ' S)- and (5 ' R)-5 ',8-Cyclo-2 '-deoxyguanosine Derivatives, Aust. J. Chem. 66, 330–335.

(47). Romieu A, Gasparutto D, Molko D, and Cadet J (1998) Site-specific introduction of (5 ' S)-5 ',8-cyclo-2 '-deoxyadenosine into oligodeoxyribonucleotides, J. Org. Chem. 63, 5245–5249.

(48). Romieu A, Gasparutto D, and Cadet J (1999) Synthesis and characterization of oligonucleotides containing 5 ',8-cyclopurine 2 '-deoxyribonucleosides: (5 ' R)-5 ',8- cyclo-2 '-deoxyadenosine, (5 ' S)-5 ',8-cyclo-2 '-deoxyguanosine, and (5 ' R)-5 ',8-cyclo-2 '-deoxyguanosine, Chem. Res. Toxicol. 12, 412–421. [PubMed: 10328751]

(49). Cosman M, Ibanez V, Geacintov NE, and Harvey RG (1990) Preparation and isolation of adducts in high yield derived from the binding of two benzo[a]pyrene-7,8- dihydroxy-9,10-oxide stereoisomers to the oligonucleotide d(ATATGTATA), Carcinogenesis 11, 1667–1672. [PubMed: 2119261]

(50). Lowary PT, and Widom J (1998) New DNA sequence rules for high affinity binding to histone octamer and sequence-directed nucleosome positioning, J. Mol. Biol. 276, 19–42. [PubMed: 9514715]

(51). Luger K, Rechsteiner TJ, and Richmond TJ (1999) Preparation of nucleosome core particle from recombinant histones, Methods Enzymol. 304, 3–19. [PubMed: 10372352]

(52). Dyer PN, Edayathumangalam RS, White CL, Bao Y, Chakravarthy S, Muthurajan UM, and Luger K (2004) Reconstitution of nucleosome core particles from recombinant histones and DNA, Methods Enzymol. 375, 23–44. [PubMed: 14870657]

(53). Rodriguez-Collazo P, Leuba SH, and Zlatanova J (2009) Robust methods for purification of histones from cultured mammalian cells with the preservation of their native modifications, Nucleic Acids Res. 37, e81. [PubMed: 19443446]

(54). Liu Y, Reeves D, Kropachev K, Cai Y, Ding S, Kolbanovskiy M, Kolbanovskiy A, Bolton JL, Broyde S, Van Houten B, and Geacintov NE (2011) Probing for DNA damage with beta-hairpins: similarities in incision efficiencies of bulky DNA adducts by prokaryotic and human nucleotide excision repair systems in vitro, DNA Repair (Amst) 10, 684–696. [PubMed: 21741328]

(55). Thastrom A, Lowary PT, and Widom J (2004) Measurement of histone-DNA interaction free energy in nucleosomes, Methods SS, 33–44.

(56). Dixon WJ, Hayes JJ, Levin JR, Weidner MF, Dombroski BA, and Tullius TD (1991) Hydroxyl radical footprinting, MethodsEnzymol. 208, 380–413.

(57). Jain SS, and Tullius TD (2008) Footprinting protein-DNA complexes using the hydroxyl radical, Nat. Protoc. 3, 1092–1100. [PubMed: 18546600]

(58). Lowary PT, and Widom J (1997) Nucleosome packaging and nucleosome positioning of genomic DNA, Proc. Natl. Acad. Sci. USA 94, 1183–1188. [PubMed: 9037027]

(59). Mann DB, Springer DL, and Smerdon MJ (1997) DNA damage can alter the stability of nucleosomes: effects are dependent on damage type, Proc. Natl. Acad. Sci. U S A 94, 2215–2220. [PubMed: 9122174]

(60). Clegg RM (1992) Fluorescence resonance energy transfer and nucleic acids, Methods Enzymol. 211, 353–388. [PubMed: 1406315]

(61). Gansen A, Hauger F, Toth K, and Langowski J (2007) Single-pair fluorescence resonance energy transfer of nucleosomes in free diffusion: optimizing stability and resolution of subpopulations, Anal. Biochem. 368, 193–204. [PubMed: 17553453]

(62). Kelbauskas L, Chan N, Bash R, Yodh J, Woodbury N, and Lohr D (2007) Sequence-dependent nucleosome structure and stability variations detected by Forster resonance energy transfer, Biochemistry 46, 2239–2248. [PubMed: 17269656]

(63). Gansen A, Toth K, Schwarz N, and Langowski J (2009) Structural variability of nucleosomes detected by single-pair Forster resonance energy transfer: histone acetylation, sequence variation, and salt effects,. JPhys. Chem. B 113, 2604–2613. [PubMed: 18950220]

(64). Kelbauskas L, Yodh J, Woodbury N, and Lohr D (2009) Intrinsic promoter nucleosome stability/dynamics variations support a novel targeting mechanism, Biochemistry 48, 4217–4219. [PubMed: 19374398]

(65). Duan MR, and Smerdon MJ (2010) UV damage in DNA promotes nucleosome unwrapping, J. Biol. Chem. 285, 26295–26303. [PubMed: 20562439]

(66). Duan MR, and Smerdon MJ (2014) Histone H3 Lysine 14 (H3K14) Acetylation Facilitates DNA Repair in a Positioned Nucleosome by Stabilizing the Binding of the Chromatin Remodeler RSC (Remodels Structure of Chromatin), J. Biol. Chem. 289, 8353–8363. [PubMed: 24515106]

(67). Tóth K, Bohm V, Sellmann C, Danner M, Hanne J, Berg M, Barz I, Gansen A, and Langowski J (2013) Histone- and DNA sequence-dependent stability of nucleosomes studied by single-pair FRET, Cytometry A 8S, 839–846.

(68). Bohm V, Hieb AR, Andrews AJ, Gansen A, Rocker A, Toth K, Luger K, and Langowski J (2011) Nucleosome accessibility governed by the dimer/tetramer interface, Nucleic Acids Res. 39, 3093–3102. [PubMed: 21177647]

(69). Bonisch C, Schneider K, Punzeler S, Wiedemann SM, Bielmeier C, Bocola M, Eberl HC, Kuegel W, Neumann J, Kremmer E, Leonhardt H, Mann M, Michaelis J, Schermelleh L, and Hake SB (2012) H2A.Z.2.2 is an alternatively spliced histone H2A.Z variant that causes severe nucleosome destabilization, Nucleic Acids Res. 40, 5951–5964. [PubMed: 22467210]

(70). Wood RD, Robins P, and Lindahl T (1988) Complementation of the xeroderma pigmentosum DNA repair defect in cell-free extracts, Cell 53, 97–106. [PubMed: 3349527]

(71). Shivji MK, Moggs JG, Kuraoka I, and Wood RD (2006) Assaying for the dual incisions of nucleotide excision repair using DNA with a lesion at a specific site, Method. Mol. Biol. 314, 435–456.

(72). Kropachev K, Kolbanovskii M, Cai Y, Rodriguez F, Kolbanovskii A, Liu Y, Zhang L, Amin S, Patel D, Broyde S, and Geacintov NE (2009) The sequence dependence of human nucleotide

excision repair efficiencies of benzo[a]pyrene-derived DNA lesions: insights into the structural factors that favor dual incisions, J. Mol. Biol. 386, 1193–1203. [PubMed: 19162041]

(73). Huang JC, Hsu DS, Kazantsev A, and Sancar A (1994) Substrate spectrum of human excinuclease: repair of abasic sites, methylated bases, mismatches, and bulky adducts, Proc. Natl. Acad. Sci. USA 91, 12213–12217. [PubMed: 7991608]

(74). Marteijn JA, Lans H, Vermeulen W, and Hoeijmakers JH (2014) Understanding nucleotide excision repair and its roles in cancer and ageing, Nat. Rev. Mol. Cell. Biol. 15, 465–481. [PubMed: 24954209]

(75). Kosmoski JV, Ackerman EJ, and Smerdon MJ (2001) DNA repair of a single UV photoproduct in a designed nucleosome, Proc. Natl. Acad. Sci. USA 98, 10113–10118. [PubMed: 11517308]

(76). Ura K, Araki M, Saeki H, Masutani C, Ito T, Iwai S, Mizukoshi T, Kaneda Y, and Hanaoka F (2001) ATP-dependent chromatin remodeling facilitates nucleotide excision repair of UV-induced DNA lesions in synthetic dinucleosomes, EMBO J. 20, 2004–2014. [PubMed: 11296233]

(77). Wang D, Hara R, Singh G, Sancar A, and Lippard SJ (2003) Nucleotide excision repair from site-specifically platinum-modified nucleosomes, Biochemistry 42, 6747–6753. [PubMed: 12779329]

(78). Yasuda T, Sugasawa K, Shimizu Y, Iwai S, Shiomi T, and Hanaoka F (2005) Nucleosomal structure of undamaged DNA regions suppresses the non-specific DNA binding of the XPC complex, DNA Repair (Amst) 4, 389–395. [PubMed: 15661662]

(79). Mocquet V, Laine JP, Riedl T, Yajin Z, Lee MY, and Egly JM (2008) Sequential recruitment of the repair factors during NER: the role of XPG in initiating the resynthesis step, Embo J. 27, 155–167. [PubMed: 18079701]

(80). Cai Y, Kropachev K, Xu R, Tang Y, Kolbanovskii M, Kolbanovskii A, Amin S, Patel DJ, Broyde S, and Geacintov NE (2010) Distant neighbor base sequence context effects in human nucleotide excision repair of a benzo[a]pyrene-derived DNA lesion, J. Mol. Biol. 399, 397–409. [PubMed: 20399214]

(81). Cai Y, Patel DJ, Broyde S, and Geacintov NE (2010) Base sequence context effects on nucleotide excision repair, J. Nucleic Acids 2010.

(82). Svedruzic ZM, Wang C, Kosmoski JV, and Smerdon MJ (2005) Accommodation and repair of a UV photoproduct in DNA at different rotational settings on the nucleosome surface, J. Biol. Chem. 280, 40051–40057. [PubMed: 16210312]

(83). Danford AJ, Wang D, Wang Q, Tullius TD, and Lippard SJ (2005) Platinum anticancer drug damage enforces a particular rotational setting of DNA in nucleosomes, Proc. Natl. Acad. Sci US A 102, 12311–12316.

(84). Huang H, Das RS, Basu AK, and Stone MP (2011) Structure of (5'S)-8,5'-cyclo-2'-deoxyguanosine in DNA, J. Am. Chem. Soc. 133, 20357–20368. [PubMed: 22103478]

(85). Huang H, Das RS, Basu AK, and Stone MP (2012) Structures of (5'S)-8,5'-Cyclo-2'-deoxyguanosine Mismatched with dA or dT, Chem. Res. Toxicol. 25, 478–490. [PubMed: 22309170]

(86). Zaliznyak T, Lukin M, and de los Santos C. (2012) Structure and stability of duplex DNA containing (5'S)-5',8-cyclo-2'-deoxyadenosine: an oxidatively generated lesion repaired by NER, Chem. Res. Toxicol. 25, 2103–2111. [PubMed: 22928555]

(87). Cai Y, Kropachev K, Terzidis MA, Masi A, Chatgilialoglu C, Shafirovich V, Geacintov NE, and Broyde S (2015) Differences in the Access of Lesions to the Nucleotide Excision Repair Machinery in Nucleosomes, Biochemistry 54, 4181–4185. [PubMed: 26091016]

(88). Cosman M, Fiala R, Hingerty BE, Amin S, Geacintov NE, Broyde S, and Patel DJ (1994) Solution conformation of the (+)-cis-anti-[BP]dG adduct opposite a deletion site in a DNA duplex: intercalation of the covalently attached benzo[a]pyrene into the helix with base displacement of the modified deoxyguanosine into the minor groove, Biochemistry 33, 11518–11527. [PubMed: 7918365]

(89). Mocquet V, Kropachev K, Kolbanovskiy M, Kolbanovskiy A, Tapias A, Cai Y, Broyde S, Geacintov NE, and Egly JM (2007) The human DNA repair factor XPC-HR23B distinguishes stereoisomeric benzo[a]pyrenyl-DNA lesions, EMBO J. 26, 2923–2932. [PubMed: 17525733]

(90). Cai Y, Patel DJ, Geacintov NE, and Broyde S (2007) Dynamics of a benzo[a]pyrene-derived guanine DNA lesion in TGT and CGC sequence contexts: enhanced mobility in TGT explains conformational heterogeneity, flexible bending, and greater susceptibility to nucleotide excision repair, J. Mol. Biol. 374, 292–305. [PubMed: 17942115]

(91). Prasad A, Wallace SS, and Pederson DS (2007) Initiation of base excision repair of oxidative lesions in nucleosomes by the human, bifunctional DNA glycosylase NTH1, Mol. Cell. Biol. 27, 8442–8453. [PubMed: 17923696]

(92). Wallace SS (2014) Base excision repair: a critical player in many games, DNA Repair (Amst) 19, 14–26. [PubMed: 24780558]

(93). Balliano AJ, and Hayes JJ (2015) Base excision repair in chromatin: Insights from reconstituted systems, DNA Repair (Amst) 36, 77–85. [PubMed: 26411876]

(94). Ye Y, Stahley MR, Xu J, Friedman JI, Sun Y, McKnight JN, Gray JJ, Bowman GD, and Stivers JT (2012) Enzymatic excision of uracil residues in nucleosomes depends on the local DNA structure and dynamics, Biochemistry 51, 6028–6038. [PubMed: 22784353]

(95). Bilotti K, Kennedy EE, Li C, and Delaney S (2017) Human 0GG1 activity in nucleosomes is facilitated by transient unwrapping of DNA and is influenced by the local histone environment, DNA Repair (Amst) 59, 1–8. [PubMed: 28892740]

(96). Bilotti K, Tarantino ME, and Delaney S (2018) Human Oxoguanine Glycosylase 1 Removes Solution Accessible 8-0xo-7,8-dihydroguanine Lesions from Globally Substituted Nucleosomes Except in the Dyad Region, Biochemistry 57, 1436–1439. [PubMed: 29341606]

(97). Beard BC, Wilson SH, and Smerdon MJ (2003) Suppressed catalytic activity of base excision repair enzymes on rotationally positioned uracil in nucleosomes, Proc. Natl. Acad. Sci U S A 100, 7465–7470. [PubMed: 12799467]

(98). Hinz JM, Rodriguez Y, and Smerdon MJ (2010) Rotational dynamics of DNA on the nucleosome surface markedly impact accessibility to a DNA repair enzyme, Proc. Natl. Acad. Sci U S A 107, 4646–4651. [PubMed: 20176960]

(99). Odell ID, Barbour JE, Murphy DL, Della-Maria JA, Sweasy JB, Tomkinson AE, Wallace SS, and Pederson DS (2011) Nucleosome disruption by DNA ligase III-XRCC1 promotes efficient base excision repair, Mol. Cell. Biol. 31, 4623–4632. [PubMed: 21930793]

(100). Hinz JM (2014) Impact of abasic site orientation within nucleosomes on human APE1 endonuclease activity, Mutat. Res. 766–767, 19–24.

(101). Sugasawa K, Okamoto T, Shimizu Y, Masutani C, Iwai S, and Hanaoka F (2001) A multistep damage recognition mechanism for global genomic nucleotide excision repair, Genes Dev. 15, 507–521. [PubMed: 11238373]

(102). Wakasugi M, and Sancar A (1998) Assembly, subunit composition, and footprint of human DNA repair excision nuclease, Proc. Natl. Acad. Sci. U S A 95, 6669–6674. [PubMed: 9618470]

(103). Reardon JT, Mu D, and Sancar A (1996) Overproduction, purification, and characterization of the XPC subunit of the human DNA repair excision nuclease, J. Biol. Chem. 271, 19451–19456. [PubMed: 8702634]

(104). Li G, and Widom J (2004) Nucleosomes facilitate their own invasion, Nat. Struct. Mol. Biol. 11, 763–769. [PubMed: 15258568]

(105). Gong F, Kwon Y, and Smerdon MJ (2005) Nucleotide excision repair in chromatin and the right of entry, DNA Repair (Amst) 4, 884–896. [PubMed: 15961354]

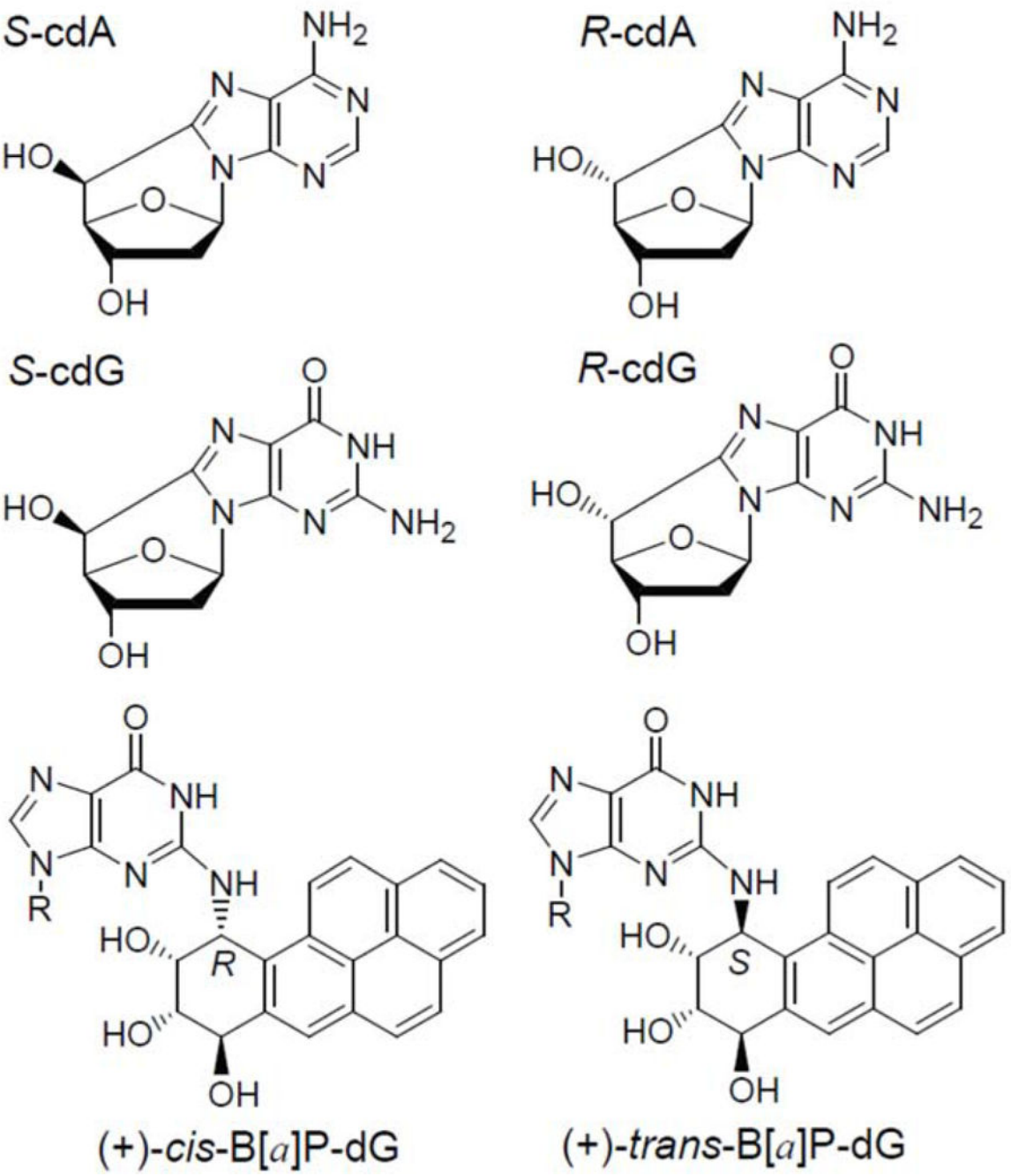

Figure 1.
Structures of the diastereomeric 5',8-cyclopurine lesions and the stereoisomeric benzo[*a*]pyrene diol epoxide-derived BPDE-dG lesions.

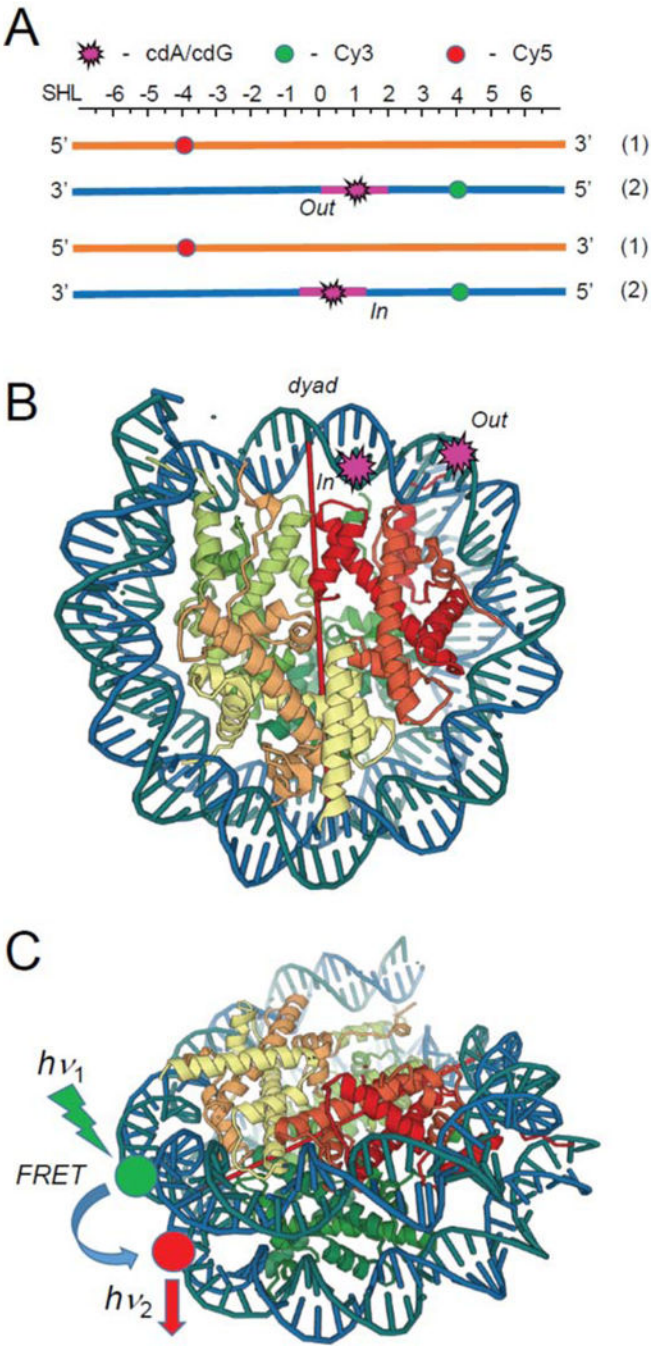

Figure 2.

(A) Schematic illustrations of the placements of the DNA lesions and the Cy3 donor and Cy5 acceptor molecules at the "*Out*" and "*In*" rotational settings in the 147-mer 601 DNA duplexes used in the FRET experiments. (B) The crystal structure of the 601 nucleosome core particles (PDB 3LZ0).[44] The dyad axis is indicated by the red line. (C) Positions of the Cy3 donor and Cy5 acceptor molecules in the nucleosome FRET experiments. The lesions were positioned at the 66-th or 70-th nt counted from the 5'-end of the 147-mer,

corresponding to the *Out* or *In* rotational settings. The internal Cy3 and Cy5 labels were positioned at nucleotides 43 and 39 counted from the dyad axis in opposite strands.

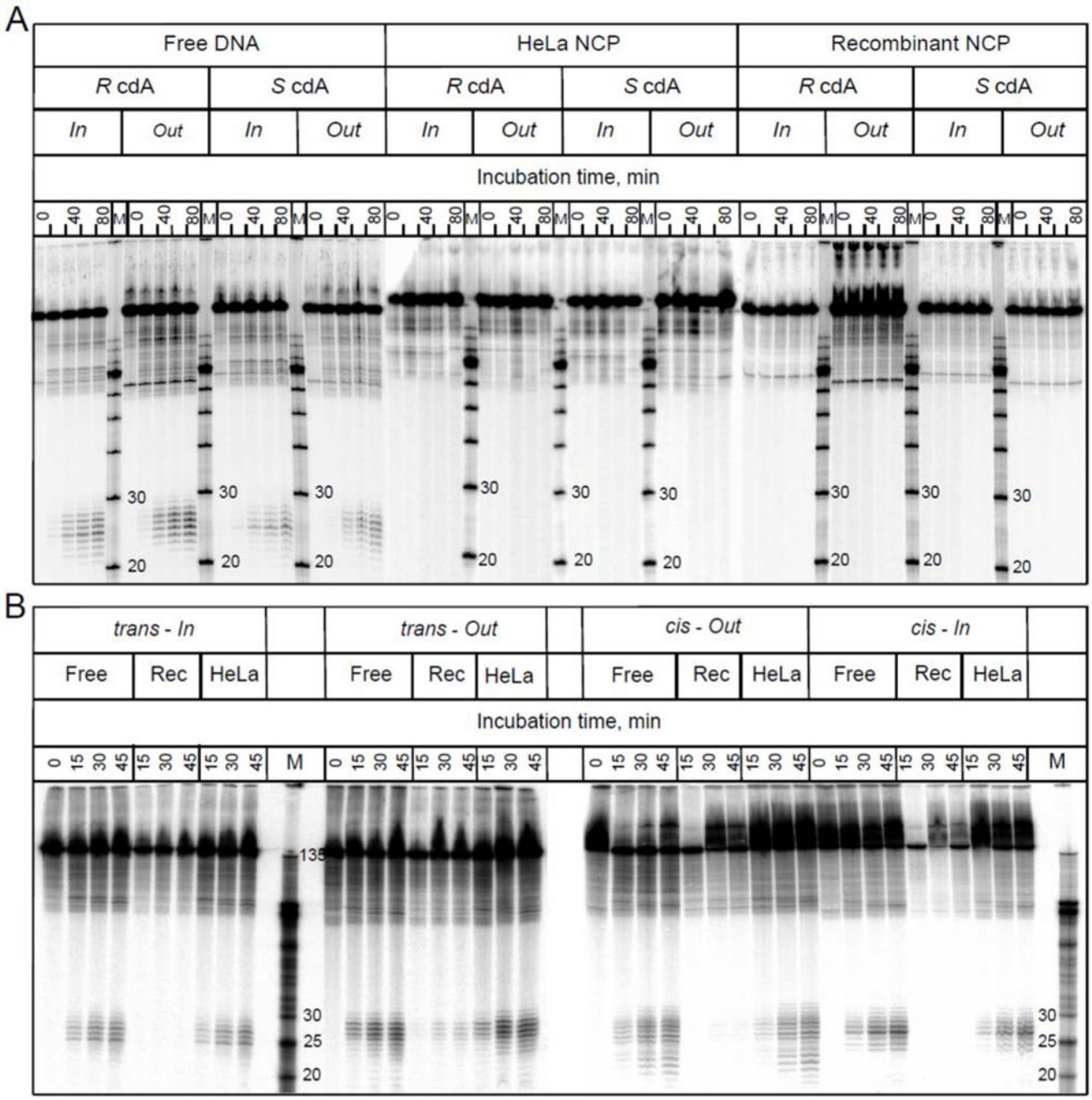

Figure 3.

Representative autoradiographs of denaturing gels of nucleotide excision experiments in HeLa cell extracts. (A) The substrates were either free 147-mer 601^{cP} DNA sequences containing single 5',8-cyclopurine lesions, or nucleosomes assembled with octamers derived from recombinant (Rec) or native, post-translationally modified histones extracted from HeLa cells. (B) Analogous NER experiments with *cis*- and *trans*-BPDE-dG adducts positioned at the same *In* and *Out* superhelical locations. Three separate gels are depicted in panels A and B.

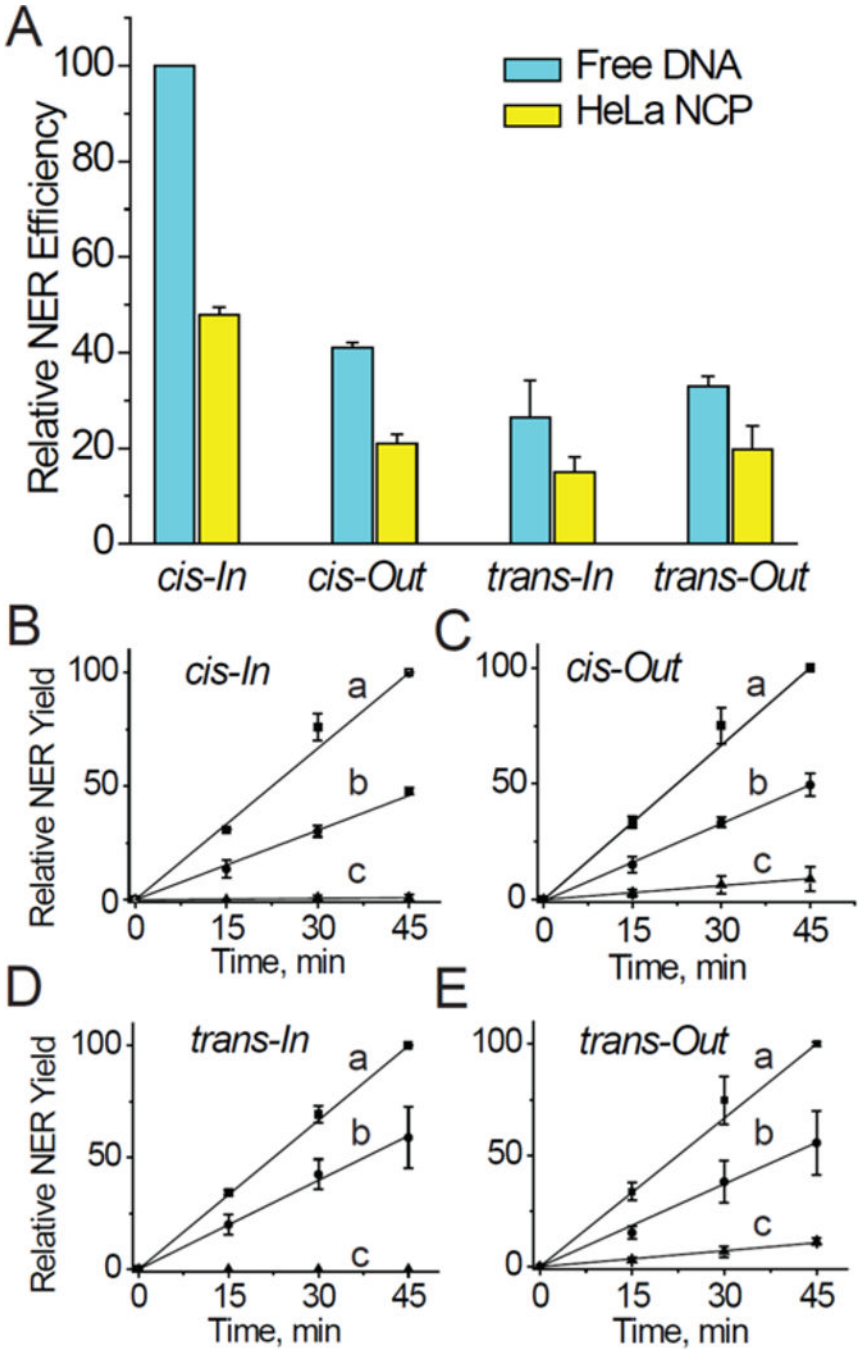

Figure 4.

(A) Comparisons of relative rates of NER dual incisions of the *cis*- and *trans*-BPDE-dG adducts embedded at the *In* or *Out* rotational settings of 147-mer free 601^{BP} DNA duplex sequences, or embedded in native HeLa histone-nucleosomes. The data points in panel A were determined from the kinetics of formation of the 24–30 nt NER dual incision products as a function of incubation time in HeLa cell extracts shown in panels B, C, D, and E (a - free DNA, b-HeLa NCP, and c–recombinant NCP). These averages and standard deviations were derived from three independent experiments, each with different nucleosome and HeLa

cell extract preparations. In each of the three sets of individual experiments, all results were expressed relative to the rate observed in the case of the free DNA *cis-In* adduct measured at the 45 min time point; the arbitrary value of 100 was assigned to these measured values because the highest NER yields were observed in each individual set of three experiments in the case of each different *cis-In* BPDE-dG adduct in free DNA (Figure 4). The NER efficiencies were dependent on the particular cell cultures and varied from ~ 4 to 12% in the case of the *cis*-BPDE-dG adducts in free DNA at the 45 min time points.

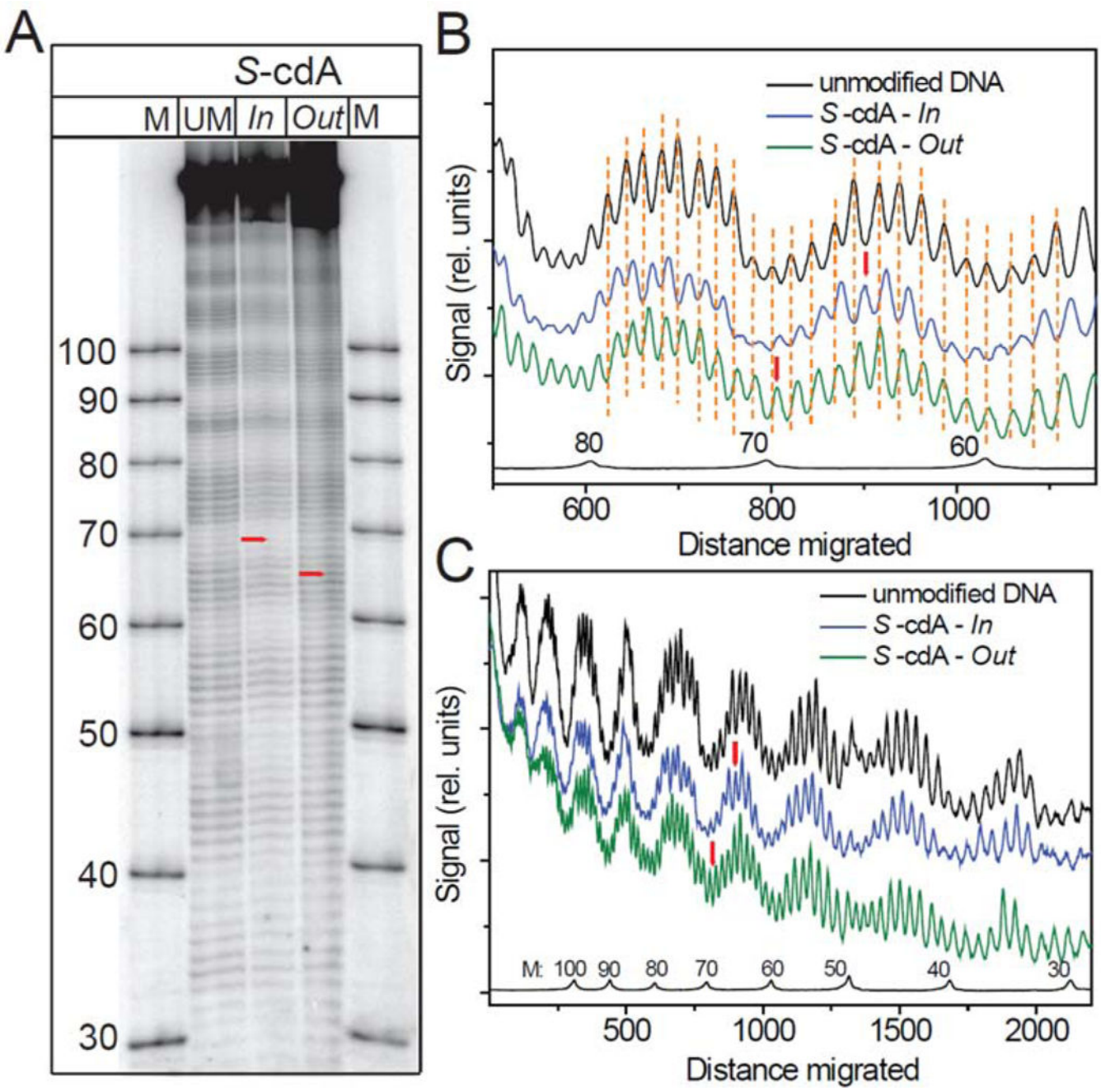

Figure 5.

Hydroxyl radical footprints obtained with recombinant histone nucleosomes assembled from the 147-mer 601^{cP} DNA sequences containing *S*-cdA lesions at the *Out* and *In* rotational settings. (A) Autoradiograph of a typical hydroxyl radical footprint experiment. (B) Scan of the results shown (A) in the region containing the lesions (red vertical bar), and (C) Scan of the entire sequence.

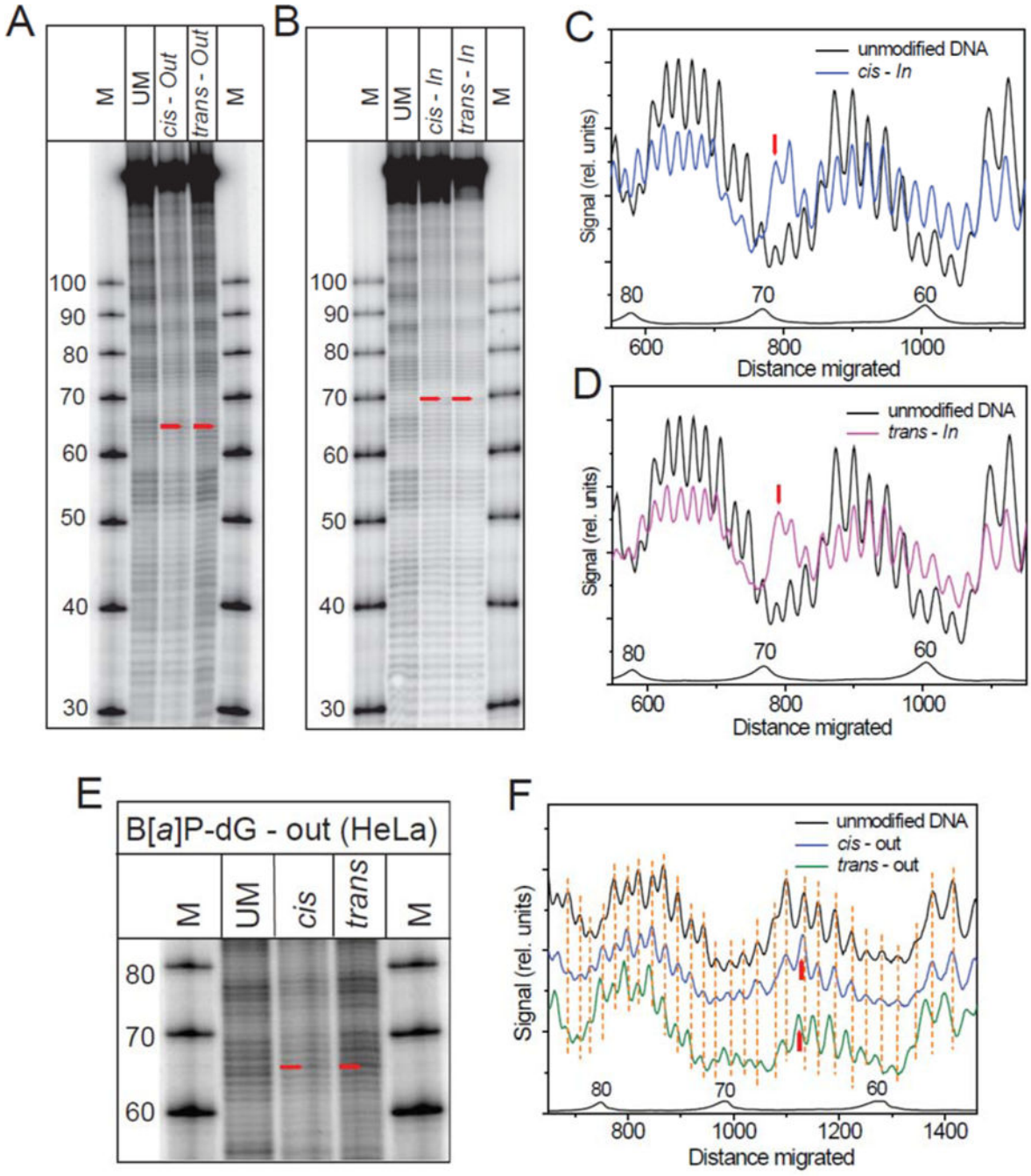

Figure 6.

Hydroxyl radical footprints obtained with HeLa histone nucleosomes assembled from 601 sequences containing *cis*-or *trans-BPDE*-dG adducts. (A) Autoradiograph with the BPDE-dG adducts at the *Out* rotational setting, (B) Autoradiograph obtained with the BPDE-dG adducts at the *In* setting. (C) Scan of the *cis-In* and unmodified DNA samples. (D) Scan of the *trans-In* and unmodified DNA samples. (E) Autoradiograph of the *cis*-and *trans*-BPDE-dG adduct samples at the *Out* rotational setting. (F) Scans of the autoradiograph in panel E.

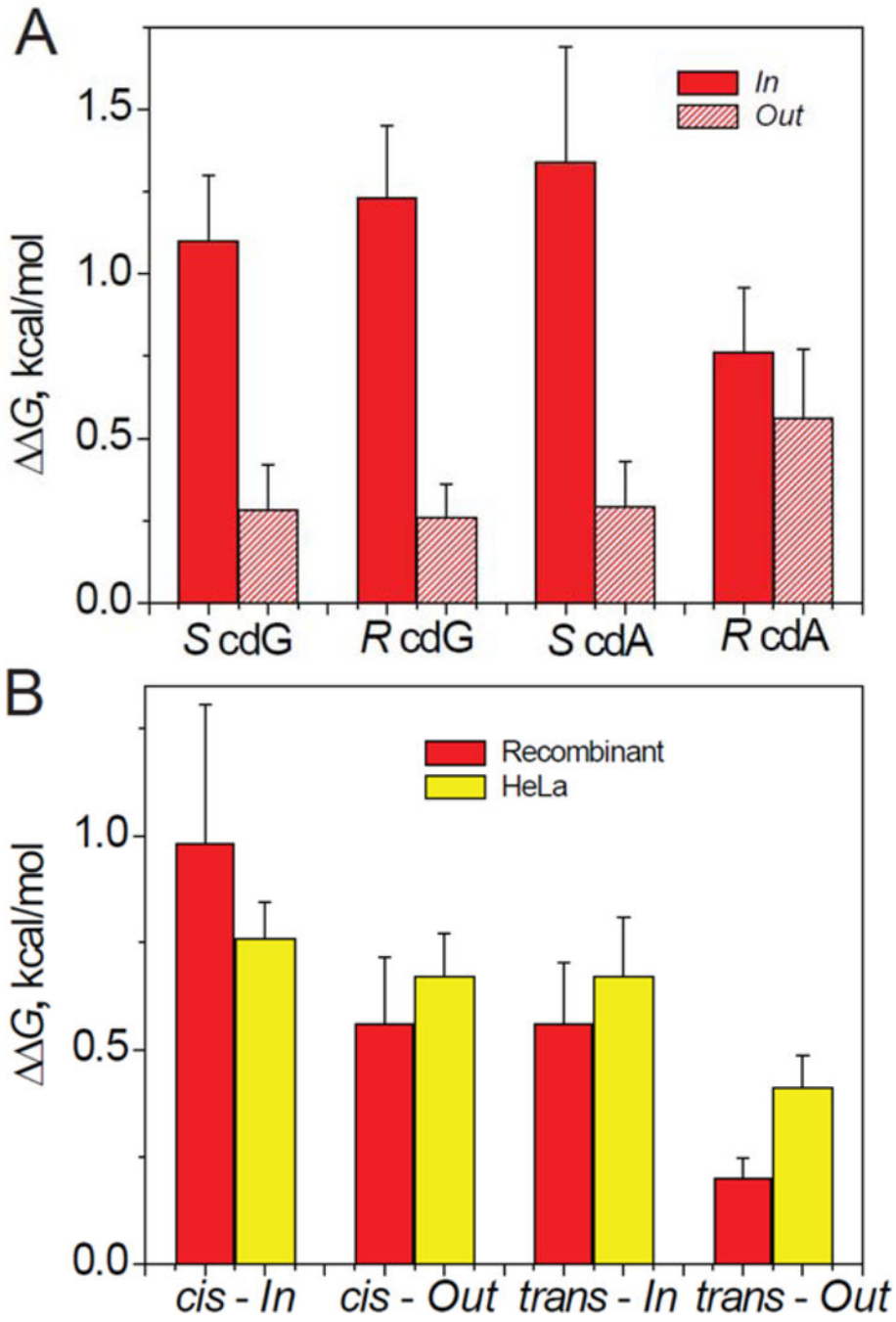

Figure 7.

(A) The relative free energies of formation of nucleosome, ($\Delta\Delta G$). The NCPs were assembled with recombinant histone octamers and 147-mer 601^{cP} Widom DNA sequences containing single 5′,8-cyclopurine lesions positioned at *In* or *Out* rotational settings. (B) The ΔΔG values determined in analogous experiments with nucleosomes assembled from 147-mer 601^{BP} DNA sequences with single BPDE-dG adducts at the *In* or *Out* rotational settings and octamers derived from recombinant or native HeLa cell histones. are close to those reported for another non-bulky DNA lesion, the cyclobutane thymine dimer (CTD, $\Delta\Delta G$ =

1.1 and 0.6 kcal/mol at the *In* and *Out* positions, respectively) also positioned near the dyad in another strong positioning sequence (TG) in native chicken erythrocyte NCPs.[82]

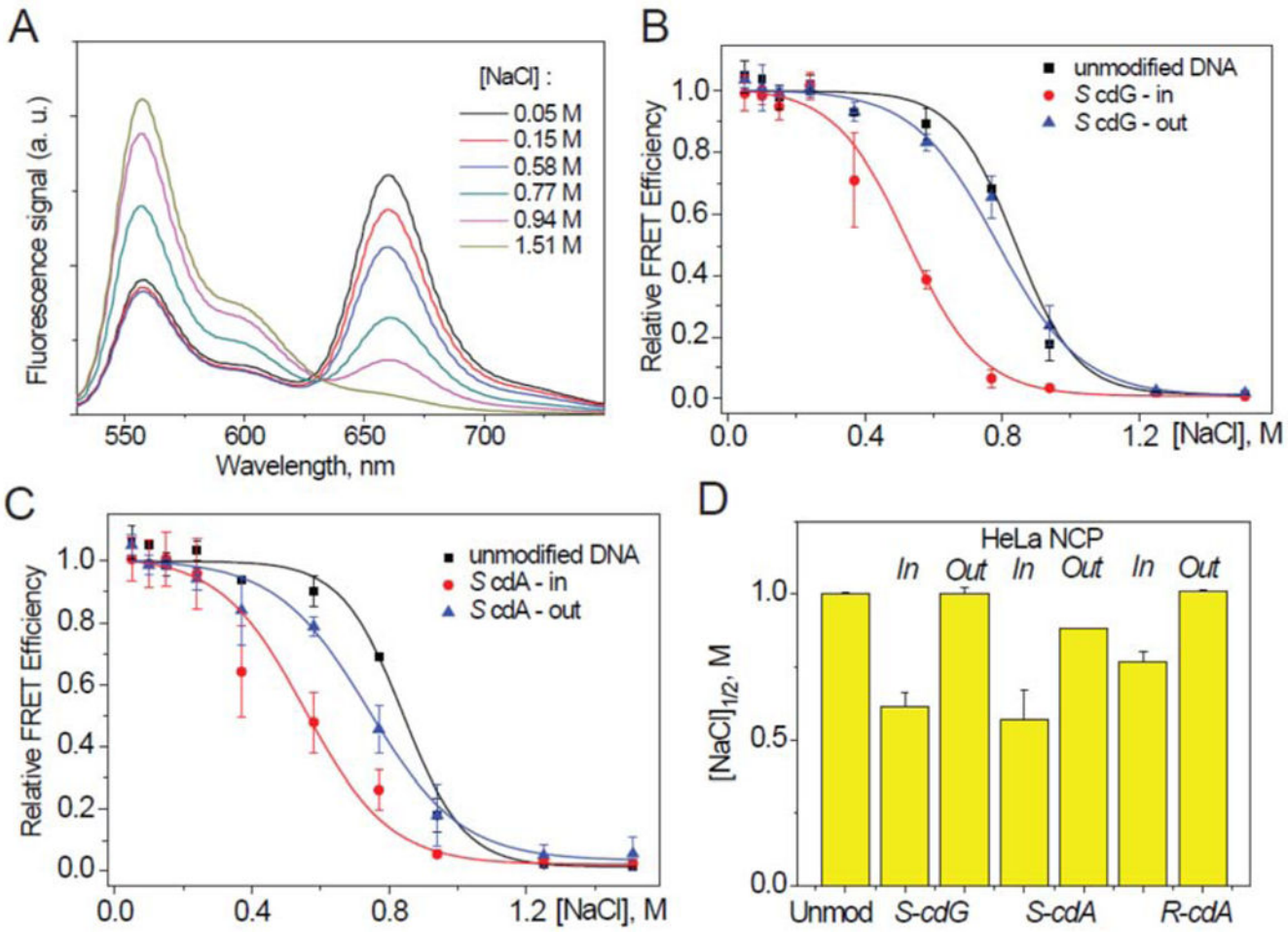

Figure 8.

Unwrapping of nucleosomes assembled with 601^{cP} 147-mer DNA with *S* cdA/cdG lesions and HeLa histone octamers as a function of NaCl concentration monitored by the FRET method. (A) Typical fluorescence emission spectra obtained with an unmodified DNA-NCP sample excited at 515 nm and recorded at different NaCl concentrations. (B) Relative FRET signals measured at 670 nm of HeLa histone nucleosomes with *S* cdG lesions (B), and with *S* cdA lesions (C) as a function of NaCl concentrations; the sigmoidal curves are plots of Eq. 3. (D) Comparison of the [NaCl]1/2 values.

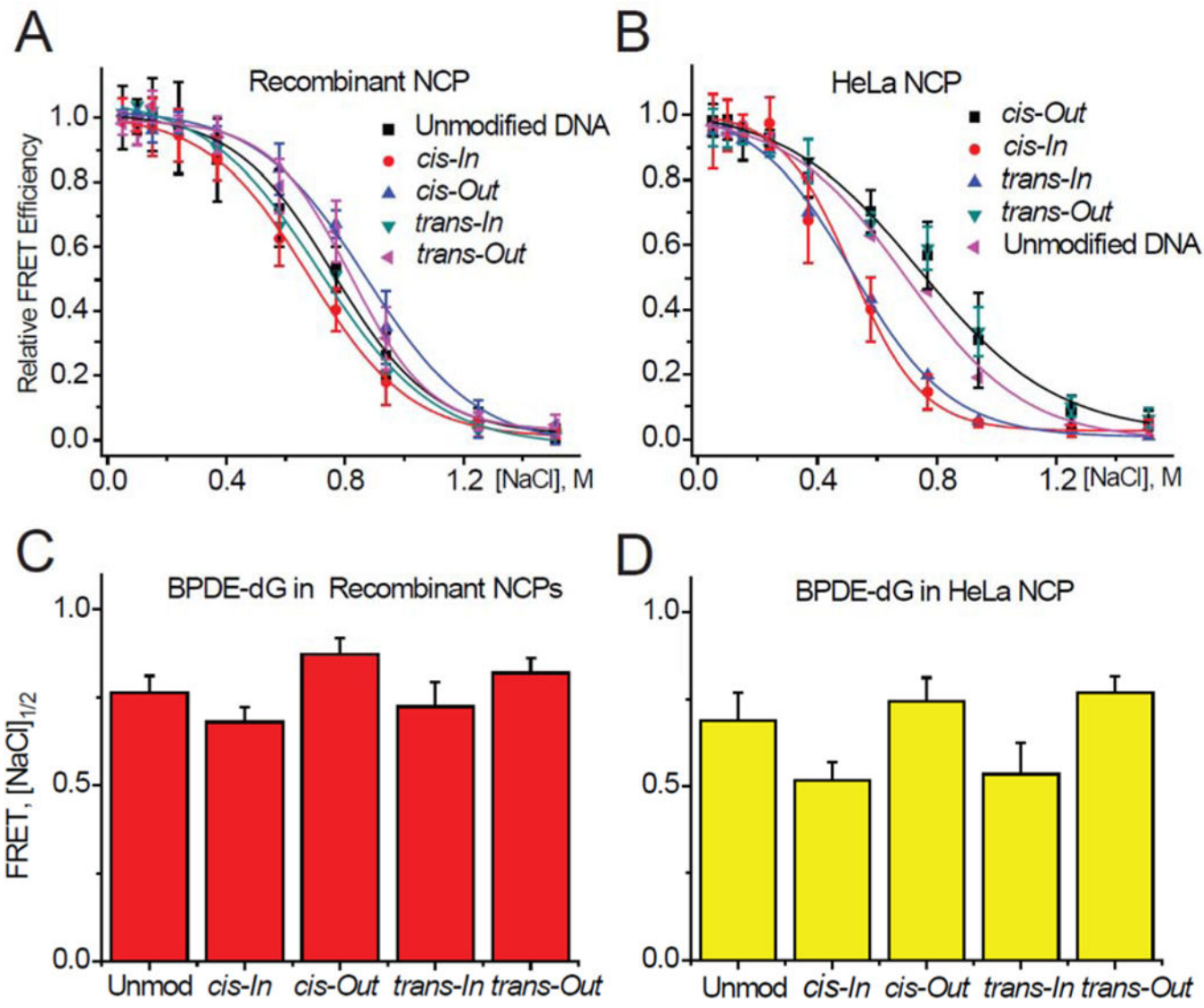

Figure 9.

FRET signals measured as a function of NaCl concentrations of 601^{BP} 147-mer DNA sequences with BPDE-dG adducts in (A) Rec-NCPs, and (B) HeLa-NCPs as a function of salt concentration. (C) and (D): Comparisons of relative nucleosome stabilities based on FRET [NaCl] 1/2 values.

Table 1.

Relative values of slopes of NER dual incision product yield formation (%NER/min) as a function of incubation time in He La cell extracts

DNA adduct	NER Free DNA*	NER HeLa-NCP*	NER Ratio Free/HeLa	NER Rec NCP*	NER Ratio Free/Rec
cis-BPDE-dG *In*	2.53±0.13	1.02±0.13	2.48±0.14	~0	
cis-BPDE-dG *Out*	2.28±0.15	1.11±0.28	2.05±0.26	0.20±0.02	11.3
trans-BPDE-dG *In*	2.43±0.08	1.02±0.05	2.38±0.06	~0	
trans-BPDE-dG *Out*	2.28±0.15	1.24±0.05	1.84±0.08	0.24±0.01	10.5
Average			2.2±0.2**		11±0.5

*Averages of three independent NER assays in different cell extracts.

**$P < 0.05$ (one-sample *t*-test).